Supplemental Information

An isochemogenic set of inhibitors to define the therapeutic potential of HDACs in beta cell protection

Florence F. Wagner[†,1], Morten Lundh[†,2,3], Taner Kaya[1], Patrick McCarren[2], Yan-Ling Zhang[1], Shrikanta Chattopadhyay[2], Jennifer P. Gale[1], Thomas Galbo[4], Stewart L. Fisher[5], Bennett C. Meier[2], Amedeo Vetere[2], Sarah Richardson[6], Noel G. Morgan[6], Dan Ploug Christensen[3], Tamara J. Gilbert[2], Jacob M. Hooker[1,7], Mélanie Leroy[1], Deepika Walpita[2], Thomas Mandrup-Poulsen[3,8], Bridget K. Wagner[*,2], and Edward B. Holson[*,1]

* Corresponding authors:

Edward B. Holson, Stanley Center for Psychiatric Research, Broad Institute of Harvard and MIT, 415 Main Street, Cambridge, MA 02142, USA

Current Address: Atlas Venture, 400 Technology Square, 10th Floor, Cambridge, MA 02139, USA; 857-201-2733; EHolson@atlasventure.com.

Bridget K. Wagner, Center for the Science of Therapeutics, Broad Institute of Harvard and MIT, 415 Main Street, Cambridge, MA 02142, USA; 617-714-7363; bwagner@broadinstitute.org.

Table of contents

Supplementary Figure S5. Simulated kinetic selectivity for CI-994 and BRD3308 at 10 mg/kg i.p. dose in mouse.

Supplementary Figure S6. Simulated target engagement profiles for HDAC 1, 2 and 3 in plasma for BRD3308 at 1 mg/kg dose i.p. (extrapolated).

Supplementary Figure S7. Toolkit compounds that do not inhibit HDAC3 do not suppress beta-cell apoptosis, as measured by caspase-3 activity.

Supplementary Figure S8. Chemical inhibition of HDAC3 prevents glucolipotoxicity-induced apoptosis in human islets – individual experiments.

Supplementary Figure S9. Confirmation of knockdown for each HDAC isoform in INS-1E cells.

Supplementary Figure S10. HDAC inhibition reduces palmitate and high glucose-induced ROS formation.

Supplementary Figure S11. BRD3308 has no effect on Bip or Xbp1s expression in response to GLT.

Supplementary Figure S12. BRD3308 reduces Atf3 and Chop expression in response to GLT.

Supplementary Figure S13. Inhibition of HDAC3 increases mitochondrial activity in glucolipotoxicity.

Supplementary Figure S14. Primer sequences for qPCR experiments.

Compound Characterization Material

Detailed Methods

Chemistry, Analog Synthesis and Characterization.

All final compounds were confirmed to be of >95% purity based on HPLC LC-MS analysis (Alliance 2795, Waters, Milford, MA). Purity was measured by UV absorbance at 210 nm. Identity was determined on a SQ mass spectrometer by positive and negative electrospray ionization. Mobile phase A consisted of 0.01% formic acid in water or pure water, while mobile phase B consisted of 0.01% formic acid in acetonitrile or pure acetonitrile. The gradient ran from 5% to 95% mobile phase B over 1.75 minutes at 1.75 mL/min. An Agilent Poroshell 120 EC-C18, 2.7 um, 3.0x30 mm column was used with column temperature maintained at 40 ^{o}C. 2.1 μL of sample solution were injected.

All reagents and solvents were purchased from commercial vendors and used as received. 1H and 13C NMR spectra were recorded on a Bruker 300 MHz or Varian UNITY INOVA 500 MHz spectrometer as indicated. Proton and carbon chemical shifts are reported in ppm (δ) relative to tetramethylsilane (δ = 0 for both 1H and 13C), CDCl3 solvent (1H δ 7.26, 13C δ 77.0) or d^6-DMSO solvent (1H δ 2.50, 13C δ 39.5). NMR data are reported as follows: chemical shifts, multiplicity (obs. = obscured, br = broad, s = singlet, d = doublet, t = triplet, m = multiplet); coupling constant(s) in Hz; integration. Unless otherwise indicated, NMR data were collected at 25°C. Flash chromatography was performed using 40-60 μm Silica Gel (60 Å mesh) on a Teledyne Isco Combiflash Rf system. Tandem Liquid Chromatography/Mass Spectrometry (LC/MS) was performed on a Waters 2795 separations module and 3100 mass detector. Analytical thin layer chromatography (TLC) was performed on EM Reagent 0.25 mm silica gel 60-F plates. Visualization was accomplished with ultraviolet (UV) light and aqueous potassium permanganate ($KMnO_4$) stain followed by heating.

*Synthesis of compound 4-acetamido-N-(2-amino-4-fluorophenyl)benzamide (**BRD3308**) as a representative procedure starting from **I** (Scheme 1 in manuscript):*

To solution of commercially available tert-butyl 2-amino-5-fluorophenylcarbamate (610 mg, 2.70 mmol) and 4-acetamidobenzoic acid (725 mg, 4.04 mmol) in DMF (2mL) at room temperature was added dropwise a solution of HATU (1.54 g, 4.04 mmol) in DMF (1 mL) then N-ethyl-N-isopropylpropan-2-amine (1.337 ml, 8.09 mmol). The resulting reaction was stirred at room temperature for 14h. The reaction was then quenched by sodium bicarbonate. Some of the desired product precipitated out of solution and was filtered off as a white solid. The remaining solution was extracted with ethyl acetate. The combined organic layers were washed with brine, then dried over sodium sulfate, filtered and concentrated. The product was purified by column chromatography (silica gel, 20-80% EtOAc/hexanes) to obtain tert-butyl 2-(4-acetamidobenzamido)-5-fluorophenylcarbamate (0.64g, 61% yield).

To a solution of tert-butyl 2-(4-acetamidobenzamido)-5-fluorophenylcarbamate (640 mg, 1.652 mmol) in dichloromethane (3 mL) at room temperature was added trifluoroacetic acid (1265 µL, 16.52 mmol). The resulting solution was stirred for 2h. The reaction was then quenched with a saturated aqueous solution of sodium bicarbonate. The desired product precipitated out of solution and was filtered. The precipitate was washed with cold EtOAc to obtain the desired product as a white solid. The aqueous phase was washed with EtOAc (3X10 mL). The combined organic layers were washed with water then brine, dried over sodium sulfate, filtered and concentrated. The product was purified by column chromatography (silica gel, 20% EtOAc/hexanes) to obtain the desired product. The combined yield was 0.29g, 61% yield of compound 1. ^{1}HNMR (300 MHz, d^{6}-DMSO): δ 10.21 (s, 1H), 9.50 (s, 1H), 7.94 (d, *J* = 8.4 Hz, 2H), 7.69 (d, *J* = 8.4 Hz, 2H), 7.10 (t, *J* = 8.1 Hz, 1H), 6.55 (dd, *J* = 2.7, 11.1 Hz, 1H), 6.36 (dt, *J* = 2.7, 8.5 Hz, 1H), 5.22 (br s, 2H), 2.09 (s, 3H); 13C NMR (300 MHz, d^{6}-DMSO): δ 168.67, 164.99, 162.51, 159.35, 145.47, 145.31, 142.07, 128.63, 128.51, 128.37, 119.46, 117.99, 102.17,

101.87, 101.63, 101.29, 24.09; HR ESI MS calcd. for C15H15FN3O2 m/z [M + H]+ calcd 288.1148, found 288.1146; HPLC purity: >99%.

*4-acetamido-N-(2-amino-4-chlorophenyl)benzamide (**9**)*

^{1}HNMR (300 MHz, d^{6}-DMSO): δ 10.21 (s, 1H), 9.53 (s, 1H), 7.93 (d, *J* = 8.4 Hz, 2H), 7.69 (d, *J* = 8.4 Hz, 2H), 7.16 (d, *J* = 8.4 Hz, 1H), 6.81 (d, *J* = 2.1 Hz, 1H), 6.59 (dd, *J* = 2.1, 8.1 Hz, 1H), 5.23 (br s, 2H), 2.09 (s, 3H); ^{13}CNMR (300 MHz, d^{6}-DMSO) δ 168.68, 164.91, 144.74, 142.15, 130.25, 128.68, 128.57, 128.13, 122.19, 117.99, 115.39, 114.78, 24.10; HR ESI MS calcd. for C15H14ClN3NaO2 m/z [M + Na]+ calcd 326.0672, found 326.0664; HPLC purity: >99%.

*4-acetamido-N-(2-amino-4-methylphenyl)benzamide (**8**)*

^{1}HNMR (300 MHz, d^{6}-DMSO): δ 9.96 (s, 1H), 9.27 (s, 1H), 7.70 (d, *J* = 8.7 Hz, 2H), 7.45 (d, *J* = 8.7 Hz, 2H), 6.78 (d, *J* = 7.8 Hz, 1H), 6.36 (br s, 1H), 6.17 (d, *J* = 8.1 Hz, 1H), 4.56 (br s, 2H), 1.96 (s, 3H), 1.86 (s, 3H); ^{13}CNMR (300 MHz, d^{6}-DMSO) δ 168.65, 164.69, 142.86, 141.99, 135.32, 128.83, 128.56, 126.50, 121.08, 118.0, 117.10, 116.53, 24.09, 20.78; HR ESI MS calcd. for C16H17N3NaO2 m/z [M + Na]+ calcd 306.1218, found 306.1221; HPLC purity: >99%.

*4-acetamido-N-(2-amino-5-(pyridin-4-yl)phenyl)benzamide (**BRD2492**)*

^{1}HNMR (300 MHz, d^{6}-DMSO): δ 10.24 (br s, 1H), 9.68 (br s, 1H), 8.51 (d, *J* = 6.0 Hz, 2H), 7.98 (d, *J* = 8.7 Hz, 2H), 7.75-7.66 (m, 3H), 7.59 (d, *J* = 6.0 Hz, 2H), 7.54-7.48 (m, 1H), 6.89 (d, *J* = 8.4 Hz, 1H), 5.38 (br s, 2H), 2.10 (s, 3H); ^{13}CNMR (300 MHz, d^{6}-DMSO) δ 168.71, 165.03, 149.98, 146.77, 144.74, 142.16, 128.72, 128.70, 125.12, 124.82, 124.15, 123.57, 119.62, 118.01, 116.23, 24.10; HR ESI MS calcd. for C20H19N4O2 m/z [M + H]+ calcd 347.1508, found 347.1511; HPLC purity: 97%.

*4-acetamido-N-(2-amino-5-methylphenyl)benzamide (**6**)*

^{1}HNMR (500 MHz, d^{6}-DMSO): δ 10.16 (s, 1H), 9.49 (s, 1H), 7.90 (d, J = 9.0 Hz, 2H), 7.67 (d, J = 8.5 Hz, 2H), 6.98 (s, 1H), 6.77 (d, J = 8.0 Hz, 1H), 6.67 (d, J = 8.0 Hz, 1H), 4.64 (br s, 2H), 2.15 (s, 3H), 2.07 (s, 3H); HR ESI MS calcd. for C16H17N3O2 m/z [M + H]+ calcd 284.1394, found 284.1395; HPLC purity: 96%.

*4-acetamido-N-(2-amino-5-fluorophenyl)benzamide (**7**)*

^{1}HNMR (500 MHz, d^{6}-DMSO): δ 10.19 (br s, 1H), 9.53 (br s, 1H), 7.92 (d, *J* = 10.5 Hz, 2H), 7.69 (d, *J* = 10.5 Hz, 2H), 7.16 (dd, *J* = 3.5, 13.0 Hz, 1H), 6.85-6.74 (m, 2H), 4.81 (br s, 2H), 2.09 (s, 3H); HR ESI MS calcd. for C15H14N3O2 m/z [M + H]+ calcd 288.1143, found 288.1143; HPLC purity: 98%.

Biochemical Assay. Materials. All HDACs were purchased from BPS Bioscience. HDAC Substrate A and Substrate B were synthesized in house according to the synthetic procedure described by Zhang *et al*.(44). All the other reagents were purchased from Sigma. Caliper EZ reader II system was used to collect all the biochemical assay data. In-vitro HDAC enzymatic endpoint assay using microfluidic capillary electrophoresis to profile HDAC inhibitors: Purified HDAC1-9 (0.5~5 nM) were incubated with 2 μM carboxyfluorescein (FAM)-labeled acetylated peptide substrate A or B and test compound for 60 min at room temperature, in HDAC assay buffer that contained 50 mM HEPES (pH 7.4), 100 mM KCl, 0.01% BSA and 0.001% Tween-20. Reactions were terminated by the addition of the known non-selective HDAC inhibitor LBH-589 (panobinostat) with a final concentration of 1.4 μM. Acetylated peptide substrate and deacetylated peptide product were separated on a Caliper LabChip EZ Reader II equipped with a 12-sipper chip in ProfilerPro separation buffer and fluorescence intensity in the substrate and product peaks was determined and analyzed using EZ Reader software (Caliper Life Sciences; Hopkinton, MA). The separation of substrate and product was performed under the following optimized conditions: upstream voltage = −500 V, downstream voltage = −1500V and pressure = −1.3 psi. The reactions were performed in duplicate for each sample. The compounds were tested in 11-point doses with 3-fold dilution in 384-well plate format. The percent inhibition was plotted against the compound concentration, and the IC50 values were calculated using Condoseo in Genedata screener.

Inhibition kinetics of CI-994, BRD2492 and BRD3308 with HDACs 1, 2, and 3 were evaluated by the progression curves in inhibition and dilution experiments(13). To determine the mechanism and associated kinetic values, a series of inhibition progression curves were generated for HDACs 1, 2 and 3 in the presence of compound at different concentrations. Kinetic reactions were assembled in 384-well microtiter plate wells by adding 1.6 nM, 1.7 nM and 0.5 nM of HDACs 1, 2, and 3, respectively, into separate reaction mixtures containing 2 μM HDAC substrate A and

compound. Plates were immediately placed into a LabChip EZ Reader whereby the wells were sampled periodically throughout a 4-h reaction period. The fluorescent product and substrate were separated and monitored on the Caliper microfluidic instrument. The conversion of substrate was calculated with Caliper software. The progression curves at different inhibitor concentrations were analyzed with a nonlinear regression program in Origin 8.5 software (Origin Lab.Inc) to the user-defined integrate rate equation for slow-binding inhibitors. The off-rate of compounds were determined from the dilution experiment. HDAC1 (0.1 μM), HDAC2 (0.1 μM) or HDAC3 (0.05 μM) were incubated with compound at 50 μM, 50 μM or 1.25 μM respectively for 1 h. The mixtures were then diluted 100-fold into buffer containing 2uM substrate A. HDAC-diluted samples were measured continuously over a 4-h period. The HDAC inhibitor off-rates were calculated from HDAC activity after dilution from inhibitor-preincubated sample compared to the non-preincubated control.

Cell culture. INS-1E (provided by P. Maechler and C. Wollheim, University of Geneva, Switzerland) were maintained in complete medium as previously described(45). For experimental procedures, culture medium with 1% FBS and 1% BSA was used. All experiments were performed within the split passage numbers 55-70. Primary neonatal rat islets were isolated from outbred 3 to 6 day-old Wistar rats (Taconic) and cultured in RPMI 1640 with 20 mmol/l HEPES buffer, 2 mmol/l L-glutamine, 0.038%, $NaHCO_3$, 100 U/ml penicillin, and 100 µg/ml streptomycin supplemented with 1% FBS. Human islets were provided by the Integrated Islet Distribution Program administered by the City of Hope Hospital (IIDP: http://iidp.coh.org/). Islets were dissociated and seeded (30,000 cells/well) into black optical 96-well plates that had previously been coated with extracellular matrix from the human HTB-9 bladder carcinoma cell line(46). The dissociated islet cell cultures were cultured in CMRL media in 10% FBS for 3 days before exposure to palmitate (0.5 mM) and high glucose (25 mM) in medium with 1% BSA and without FBS for 72 h.

Cell viability assays. INS-1E cells (5,000 cells/well) were seeded in white optical 384-well plates (Corning Life Sciences) with 50 μL complete medium. After overnight incubation, cells were exposed to 50 μL medium per well with palmitate, glucose, and HDAC inhibitors. After 48 or 72 h, medium was removed and MTT assays were performed. Alternatively, 20 μL or 100 μL Caspase-Glo 3/7 reagent was added to INS-1E or human islets, respectively. After two-h incubation at room temperature, luminescence was measured using an Envision plate reader (PerkinElmer). Unless otherwise stated, each condition was assayed in 6-14 biological replicates. Rat islets (50 islets/well) were cultured in 48-well plates (NUNC) and exposed to palmitate (0.5 mM) and glucose (25 mM) in medium supplemented with 1% FBS and 1% BSA for 60 h. Cell death was determined in biological duplicates using a cell death ELISA assay (Roche).

Real-time PCR. INS-1E cells were seeded in 6-well plates (one million/well) in complete medium. After two days, medium was removed and cells were exposed to the indicated concentrations of palmitate, glucose, HDAC inhibitors, or vehicle. RNA was isolated using an RNeasy kit (Qiagen) according to the manufacturer's instructions, cDNA synthesis was performed according to manufacturer's guidelines (Qiagen, Applied Biosystems), and real-time PCR using the SYBR green detection method (Applied Biosystems). Each cDNA sample in triplicate was subjected to two individual PCR amplifications, either for the gene of interest or the reference gene β-actin. Primer sequences used in this study are listed in **SI Appendix, Fig. S14**.

Immunoblotting. Treated cells were lysed using Passive Lysis Buffer (Promega) containing protease inhibitors (Roche). Lysates were adjusted for protein concentration (Bradford), proteins separated by SDS-PAGE, and transferred to a PVDF membrane. Primary antibodies were from Cell Signaling Technology, Signalway Antibody, Millipore, Sigma, and Santa Cruz. Secondary antibodies were horseradish peroxidase-coupled, and blots were developed using a chemiluminescence detection system (SuperSignal; BioVision). Light emission was captured using an Imaging Station 4000MM (Carestream) or an ImageGuage 4.0 (Fujifilm). Total protein levels were normalized to β-actin (for liver) or GAPDH (for muscle). Phosphorylation levels of individual proteins were normalized to the total amounts of the respective proteins.

Insulin assay. INS-1E cells were seeded in 96-well plates (20,000 cells/well) and the next day, cells were exposed to 100 μL medium/well with the indicated concentrations of palmitate, glucose, HDAC inhibitors, or vehicle. After 48 h, medium was removed and cells were incubated for 2 h in KRBH buffer (135 mM NaCl, 3.6 mM KCl, 5 mM $NaHCO_3$, 0.5 mM NaH_2PO_4, 0.5 mM $MgCl_2$, 1.5 mM $CaCl_2$, 10 mM HEPES, pH 7.4, 0.1% BSA) lacking glucose. Cells were subsequently incubated with KRBH buffer containing 2 mM or 16 mM glucose for 1 h. Supernatants were collected for measurement of insulin. For measuring insulin content, cells were washed in PBS and lysed using Passive Lysis Buffer. Insulin was measured with a rat insulin ELISA kit (Alpco). Total insulin content was normalized to total protein (Bradford assay). Each condition was assayed in biological duplicate.

***ROS formation*.** INS-1E cells were seeded in 96-well plates (50,000 cells/well). Two days after incubation, media was removed and cells exposed to 100 μL medium/well with the indicated concentrations of palmitate, glucose, HDAC inhibitors, or vehicle. After 24 h, cells were aspirated and incubated for 45 min in phenol red-free RPMI (Invitrogen) containing 10 μM CM-H_2DCFDA probe (Invitrogen). Wells were subsequently washed twice with phenol red-free RMPI, incubated for 3 min with Hoechst 33342 (10 μg/mL) in phenol red-free media, followed by a last wash step. Fluorescence was captured by an IX-Micro automated fluorescence microscope (Molecular Devices) and quantification of ROS per cell was analyzed using MetaXpress software. Each condition was assayed in five biological replicates.

***RNA interference*.** Small-interfering RNAs against Hdac1, Hdac2 and Hdac3 were from Dharmacon (Thermo Scientific). siRNAs (final concentration of 25 nM) were transfected into INS-1E cells (5,000/well for caspase-3 activity, 1 million/well for immunoblotting) for 8 h using DharmaFECT reagent (Thermo Scientific). Transfected cultures were cultured for 48 h before being collected for assays.

Pancreas specimens

Subjects Six human pancreases removed at autopsy from patients with type 2 diabetes were employed in the study. The cases were selected randomly from within a previously described collection of type 2 diabetes. Specimens had been fixed in buffered formalin or unbuffered formal saline, and they were all paraffin-embedded. The selected cohort consisted of patients with a mean age of 59.3±3.6 years (range 47 to 70 years). Controls were 6 non-diabetic pancreases, age-matched to the cases with type 2 diabetes, such that they had a mean age of 60.8±3.8 years (range 46 to 69 years).

Immunohistochemistry Serial sections (4 μm) were cut from each case and mounted on glass slides coated in (3-Aminopropyl)-triethoxysilane (Sigma, Dorset, UK). Sections were processed and labeled using a standard immunoperoxidase technique for paraffin sections. HDAC antigens were unmasked by heat-induced epitope retrieval in 10 mM citrate buffer pH 6.0. Primary antibodies (Abcam, Cambridge, UK) were applied for 1 h at room temperature, with the exception of anti-HDAC3 which was incubated overnight at 4°C. Dako REAL™ Envision™ Detection System (Dako, Cambridge, UK) was used for antigen detection. Some slides were processed in the absence of primary antibody or with isotype control antisera to confirm the specificity of labeling. An arbitrary scoring system was developed to assess the intensity of staining, and the type 2 diabetes and non-diabetic control slides were examined and scored independently by two observers. The staining intensity for each of 6 islets in each case was recorded and mean values were calculated.

Donor Information

T2D	Clinical Info	Sex	Age
261/67	Recently diagnosed died of hypoglycaemia	F	46
38/66	diabetes of 3/12 duration	M	56
150/87	myocardial infarction and T2D	F	58
230/66	newly diagnosed, diverticulitis	M	69
67/71	Gastric cancer and diabetes	F	67
386/66	T2D for 1yr	F	69

NDA	Clinical Info	Sex	Age
330/71	Post op death; Cushing syndrome	M	47
110/96	Fibrosing Alveolitis	F	58
186/74	SLE	F	55
64/67	Gall Bladder Cancer	F	69
424/67	Post-op death colon cancer	M	70
77/6/87	Pneumonia	F	57

***Human megakaryocyte toxicity assay*.** Proliferation and differentiation of human megakaryocytes from undifferentiated hematopoietic multipotential stem cells was done using the MegaCult®-C Complete Kit with Cytokines (Stem cell Technologies, Vancouver Canada). Frozen human CD34+ bone marrow hematopoietic progenitors from healthy volunteers were purchased from Lonza (Walkersville, MD). Cells were thawed following the supplier's recommendations and mixed on ice with collagen-containing semi-solid low-serum culture media supplemented with recombinant human thrombopoietin, IL6 and IL3 at a final density of 5000 cells/mL. HDAC inhibitors dissolved in DMSO were added to the mixture (final DMSO concentration was 0.1% for compound concentrations ≤10 μM; 0.2 % for compound concentration 20 μM) and each mixture was plated in duplicate in chamber glass slides. After a period of 12 days of incubation at 37C when individual progenitors had proliferated into multi-cellular colonies, cultures were dehydrated and fixed with a 1:3 methanol:acetone solution. Fixed slides were blocked with 5% human serum then stained with a primary antibody recognizing the human megakaryocyte marker Glycoprotein IIb/IIIa (CD41). Secondary antibody conjugated with alkaline phosphatase followed by color reaction with Sigmafast Red TR/Naphthol was used to stain positive colonies red. Evans Blue nuclear counterstaining stained nuclei blue. Colony forming units-megakaryocyte (CFU-Mk) were quantified by using a counting grid and manually counting groups of cells with red membrane staining and blue nuclei.

***Statistical analysis*.** Comparisons between groups were by two-tailed Student's t-test or ANOVA with or without Tukey- or Dunnet-corrected *post hoc* test as appropriate. Data were analyzed using either GraphPad Prism version 6 or SAS 9.1. *p*-values less than 0.05 were considered statistically significant.

Target Engagement Simulation Protocol:

Simulated pharmacokinetic profiles of the systemic free inhibitor concentration were prepared based on the parameters obtained using non-compartmental pharmacokinetic modeling (See Supplementary Figure S3) and visual inspection to ensure goodness of fit to the experimental data. Intracellular compound concentrations were assumed to be in rapid equilibrium with and equal to the fraction unbound in plasma. The simulated pharmacokinetic profiles were then used to calculate the intracellular enzyme species according to Scheme I, through a system of differential equations (Eq 1-4). The system was assumed to be in rapid equilibrium between E and ES, while the inhibition complex EI was driven by the rate constants k_{on} and k_{off}, respectively (Eq 4). Total enzyme concentration (E_0) was fixed over the course of all simulations and the intracellular enzyme concentration was estimated for each isoform according to Wagner et al, Chemical Science, 2014 ([HDAC1] = 0.57 μM, [HDAC2] = 0.74 μM, [HDAC3] = 2.0 μM). Since the specific substrate concentrations and K_m values for each isoform are undefined, these values were assumed to be equivalent ($[S]/K_m = 1$). The kinetic parameters k_{on}, k_{off} were obtained from in vitro activity assessments (Figure 2a). Target engagement was determined as the fraction of the inhibited species relative to the total enzyme concentration (Eq 5) and plotted as a function of time.

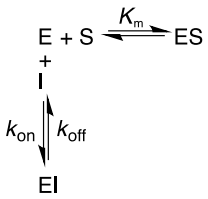

Scheme I.

$$[E_0] = [E]_{RE} + [EI] \quad (1)$$

$$\frac{dES}{dt} = [E]_{RE} \cdot \frac{{}^{[S]}/_{K_m}}{\left(1 + {}^{[S]}/_{K_m}\right)} \quad (2)$$

$$\frac{dE}{dt} = [E]_{RE} - [ES] \quad (3)$$

$$\frac{dEI}{dt} = k_{on} \cdot [E] \cdot [I] - k_{off} \cdot [EI] \quad (4)$$

$$\%TE = \frac{[EI]}{[E_0]} \cdot 100 \quad (5)$$

where:

$[E]_{RE}$ = Concentration of free enzyme in rapid equilibrium with substrate

$[E_0]$ = Total enzyme concentration

[EI] = Slow binding inhibitor:enzyme complex

[ES] = Enzyme:Substrate complex, in rapid equilibrium with free enzyme

[I] = Inhibitor concentration

[S] = Concentration of substrate

K_m = Michaelis constant of substrate binding

k_{on} = Inhibitor binding rate constant

k_{off} = Enzyme:inhibitor slow binding complex dissociation rate constant

TE = Target engagement level

General procedure for pKa determination by spectrophotometry

Reagents. The titrants used are standardized hydrochloric acid (0.5000N, J.T. Baker) and potassium hydroxide (0.5N, J.T. Baker), standardized using potassium acid phthalate (J.T. Baker). Water saturated octanol (Sigma) is used for partition experiments. ACS or HPLC grade solvents such as methanol, DMSO, and dioxane may be used for pKa determination and the solutions are kept at constant ionic strength of 0.15M KCl. Spectrophotometric experiments are carried out in the presence of a mid-range buffer solution (2.5 x 10-4 M potassium dihydrogen phosphate, Sigma) to maintain the selected pH change per titrant addition.

Procedure. The titrants are standardized using NIST traceable standards to four decimal places. The base is standardized with potassium acid phthalate in triplicate from titrations using about 0.17 grams. The acid is bought standardized to four decimal places and is standardized along with the pH electrode. The electrode is standardized everyday from pH 1.8 to 12.2. The pKa is first determined by weighing approximately 1 mg of pure drug substance into an assay vial. Ionically strength adjusted (0.15M KCl) water is added to dissolve the compound followed by an acid or base titrant addition to drop or raise the pH to the desired starting point. The solution is then titrated with acid or base to the final pH. Approximate pKa values are displayed and later refined to exact data. Assay vials are thermostated at 25°C. Up to three titrations may take place in one vial. For drug substances that are sparingly soluble in water, the pKa is determined in mixtures of water and cosolvent. The cosolvent of choice is that solvent in which the compound is soluble. A minimum of three ratios of water/cosolvent is titrated to obtain the psKa (apparent pKa in the presence of cosolvent). The aqueous pKa is determined by extrapolation using the Yasuda- Shedlovsky technique.

The spectrophotometric method uses a fiber optics dip probe, a UV light source (pulsed deuterium lamp), and a photodiode array detector to automatically capture the absorption spectra of a sample solution in the course of an acid or base titration. The compound to be analyzed must contain chromophore(s) in proximity to the ionization center(s) such that the optical properties of

the sample solution vary as a function of pH. Up to a 10 mM stock solution is prepared by dissolving 0.5-several mg of sample in 0.5-1 ml water or cosolvent. An adequate amount of stock is pipetted into the vial for titration. The dip probe is in the assay vial and 0.15 M KCl water is added to cover the dip probe. Acid or base is added to bring the pH to the desired starting point. Over the chosen pH range, the spectral changes due to ionization are captured by the photodiode array detector for subsequent analysis. Target Factor Analysis (TFA) is applied to deduce the pKa values of the sample and resolve the molar absorptivity spectra of the reacting species.

Supplementary Figure S1. Known HDAC inhibitors

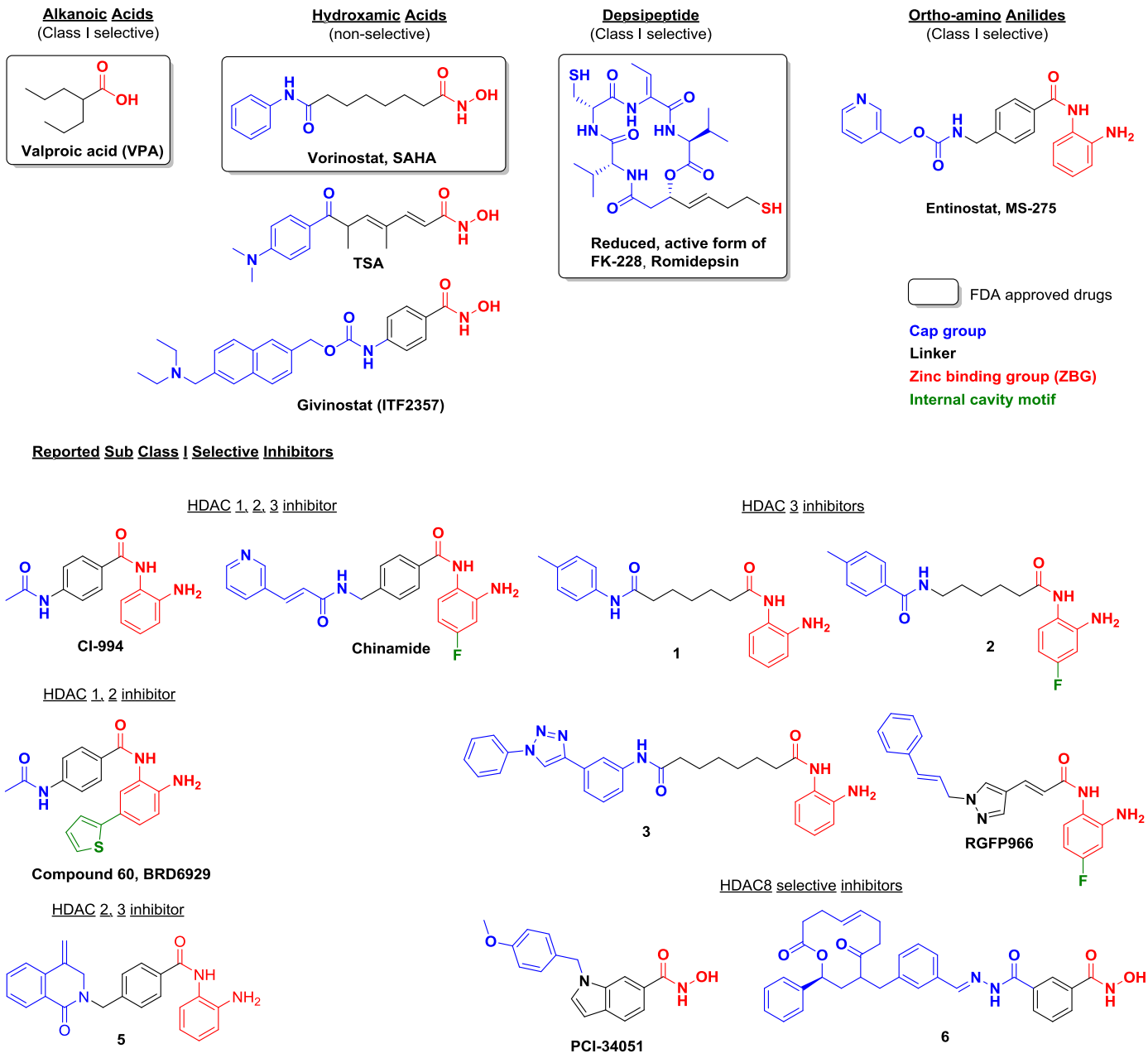

Supplementary Table S1. Compound IC_{50}'s for HDAC 1-9.

	IC50 (μM)								
Name	**HDAC1** 3h Preinc	**HDAC2** 3h Preinc	**HDAC3** 3h Preinc	**HDAC4** 0h Preinc	**HDAC5** 0h Preinc	**HDAC6** 0h Preinc	**HDAC7** 0h Preinc	**HDAC8** 0h Preinc	**HDAC9** 0h Preinc
LBH-589	0.001 ± 0.000005	0.002 ± 0.0001	0.002 ± 0.0002	0.373 ± 0.037	0.092 ± 0.021	0.002 ± 0.0001	2.83 ± 0.135	0.231 ± 0.003	2.68 ± 0.364
SAHA	0.004 ± 0.0001	0.011 ± 0.0005	0.003 ± 0.0005	>33.3	8.75 ± 1.80	0.002 ± 0.0002	>33.3	1.02 ± 0.187	>33.3
CI-994	0.041 ± 0.012	0.147 ± 0.066	0.046 ± 0.018	>33.3	>33.3	>33.3	>33.3	>33.3	>33.3
BRD2492	0.002 ± 0.001	0.019 ± 0.011	2.08 ± 0.679	>33.3	>33.3	>33.3	>33.3	>33.3	>33.3
BRD3308	1.08 ± 0.44	1.15 ± 0.38	0.064 ± 0.022	>33.3	>33.3	>33.3	>33.3	>33.3	>33.3

Supplementary Table S2. CI-994's in vitro safety and toxicological evaluation.

Selectivity profile against 80 biological targets (top 4 hits shown)		
	Target	%Inhibition at 10 μM
	A3 (adenosine)	59% (IC_{50} 4.6μM)
	Na channel	28%
	CCK_2 (Cholecytokinin)	17%
	PAC_1 (PACAP)	15%
Selectivity profile against other zinc base hydrolases		
Safety/Selectivity profile for CI-994: In vitro cytotoxicity, mutagencity, genotoxicity and hERG.		
Bacterial Cytotoxicity (Strain TA98 and TA100):	No effect @ 100 μM, 96 h incubation in either strain	
Mutagenicity (AMES) :	No effect @ 100 μM in TA98 or TA 100, 37 °C, 96 h incubation	
	No effect @ 100 μM with metabolic activation in TA98 or TA100 (rat S9 liver microsomes), 37 °C, 96 h incubation	
Genotoxicity (Micronucleus):	No Effect @ 500 μM, 37 °C, 20-24 h incubation	
	No Effect @ 500 μM, with metabolic activation (rat S9 liver microsomes) for 4 h, washed and incubated for additional 20 h at 37 °C.	
hERG (automated patch clamp	IC50 > 100 μM 28% inhibition of tail current @ 100 μM	

Top 4 hits shown. Screen included transmembrane and soluble receptors, ion channels and monoamine transporters (dopaminergic, kinases, GPCR, etc…).

In vitro pharmacology, binding assay list:
A1(*h)* (agonist radioligand)
A2A(*h)* (agonist radioligand)
A3(*h)* (agonist radioligand)
alpha1 (antagonist radioligand)
alpha2 (antagonist radioligand)
beta2(*h)* (agonist radioligand)
beta1(*h)* (agonist radioligand)
AT1(*h)* (antagonist radioligand)
BZD (central) (agonist radioligand)
BB (non selective) (agonist radioligand)
B2(*h)* (agonist radioligand)
CGRP(*h*) (agonist radioligand)
CB1(*h)* (agonist radioligand)
CCK1(*h)* (CCKA) (agonist radioligand)
CCK2(*h)* (CCKB) (agonist radioligand)
D1(*h)* (antagonist radioligand)
D2S(*h)* (agonist radioligand)
D3(*h)* (antagonist radioligand)
D4.4(*h)* (antagonist radioligand)
D5(*h)* (antagonist radioligand)
ETA(*h)* (agonist radioligand)
GABA(non-selective) (agonist radioligand)
GAL1(*h)* (agonist radioligand)
GAL2(*h)* (agonist radioligand)
PDGF (agonist radioligand)
CXCR2 (IL-8B) (*h)* (agonist radioligand)
TNF-alpha (*h*) (agonist radioligand)
CCR1(*h)* (agonist radioligand)
H1(*h)* (antagonist radioligand)
H2(*h)* (antagonist radioligand)
MC4(*h)* (agonist radioligand)
MT1 (ML1A) (*h)* (agonist radioligand)
M1(*h)* (antagonist radioligand)
M2(*h)* (antagonist radioligand)

M3(*h)* (antagonist radioligand)
M4(*h)* (antagonist radioligand)
M5(*h)* (antagonist radioligand)
NK1(*h)* (agonist radioligand)
NK2(*h)* (agonist radioligand)
NK3(*h)* (antagonist radioligand)
Y1(*h)* (agonist radioligand)
Y2(*h)* (agonist radioligand)
NTS1 (NT1) (*h)* (agonist radioligand)
delta2 (DOP) (*h)* (agonist radioligand)
kappa (KOP) (*h)* (agonist radioligand)
mu (MOP) (*h)* (agonist radioligand)
NOP (ORL1) (*h)* (agonist radioligand)
PAC1 (PACAP) (*h*) (agonist radioligand)
PPAR gamma(*h*) (agonist radioligand)
PCP (antagonist radioligand)
EP4(*h)* (agonist radioligand)
TP(*h*) (antagonist radioligand)
IP (PGI_2)(*h*) (agonist radioligand)
P2X (agonist radioligand)
P2Y (agonist radioligand)
5-HT1A(*h)* (agonist radioligand)
5-HT1B(*h)* (antagonist radioligand)
5-HT2A(*h)* (antagonist radioligand)
5-HT2B(*h)* (agonist radioligand)
5-HT2C(*h)* (antagonist radioligand)
5-HT3(*h)* (antagonist radioligand)
5-HT5a(*h)* (agonist radioligand)
5-HT6(*h)* (agonist radioligand)
5-HT7(*h)* (agonist radioligand)
Sigma (non selective) (agonist radioligand)
sst (non-selective) (*h)* (agonist radioligand)
GR(*h*) (agonist radioligand)
VPAC1 (VIP1) (*h)* (agonist radioligand)
V1a(*h)* (agonist radioligand)
Ca2+- L (verapamil site) (phenylalkylamine) (antagonist radioligand)
Kv channel (antagonist radioligand)
SKCa channel (antagonist radioligand)
Na+ channel Na+- site 2 (antagonist radioligand)
Cl- channel (GABA-gated) (antagonist radioligand)
norepinephrine transporter(*h)* (antagonist radioligand)
dopamine transporter(*h)* (antagonist radioligand)
5-HT transporter (antagonist radioligand)

Zinc-based hydrolases:
ACE(*h*)
Neutral endopeptidase
MMP-1(*h*)
MMP-2(*h*)
MMP-3(*h*)
MP-12(*h*)
MT1-MMP(*h*)
TACE(*h*)

Supplementary Figure S2. Physicochemical and ADME properties.

Compound	MW ($g.mol^{-1}$)	log P	clog D	PSA (Å)	PBS solubility (µM)	Plasma Protein Binding (% bound; **human**, *mouse*, rat)	Plasma Stability (% remaining; **human**, *mouse*, rat)	Liver Microsome Stability at 60 min (% remaining; **human**, *mouse*, rat)
CI-994	269.1	0.97	1.15	84	272	**31%**, *18%*, 53%	**100%**, *92%*, 108%	**88%**, *88%*, 105%
BRD4097	283.2	1.33	1.29	84	288	**46%**, *39%*	**100%**, *92%*	not measured
BRD2492	346.2	1.84	1.75	97	12	**83%**, *79%*, 99%	**92%**, *54%*, 98%	**78%**, *62%*, 103%
BRD3308	287.1	1.17	1.23	84	154	**40%**, *32%*, 51%	**88%**, *105%*, 99%	**82%**, *89%*, 102%

Supplementary Figure S3. Time-concentration curves in mouse plasma and calculated pharmacokinetic parameters following i.p. injection (10 mg/kg).

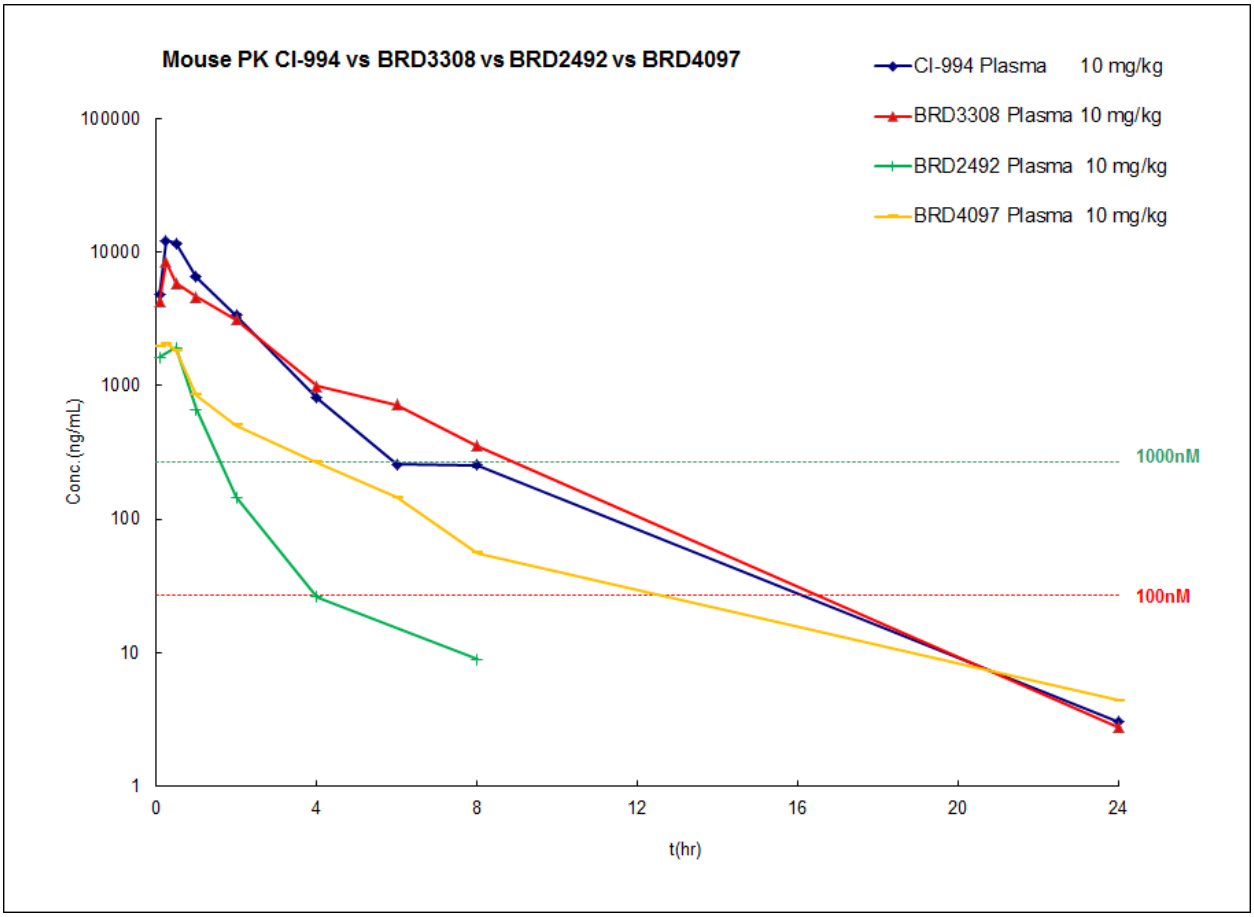

		Plasma		
		AUC Plasma	$T_{1/2}$ Plasma	Cmax Plasma
		µmol/L.hr	hr	µmol/L
CI-994	10 mg/kg	81.46	2.58	45.66
BRD3308	10 mg/kg	67.23	2.26	29.50
BRD2492	10 mg/kg	6.1	1.59	5.57
BRD4097	10 mg/kg	14.6	3.56	7.26

Supplementary Table S3. HDAC IC_{50} values and Binding Kinetics for Compound 60.

	Compound 60		
	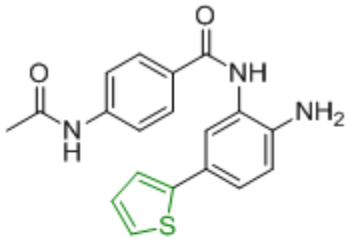		
	HDAC1	**HDAC2**	**HDAC3**
IC_{50} (μM) (3hr preincubation)	0.001 ± 0.001	0.013 ± 0.009	0.398 ± 0.105
K_{on} ($min^{-1}.\mu M^{-1}$)	1.2	0.077	-
K_{off} (min-1)	<0.00028	0.00012	0.0057
$T_{1/2}$ (min)	>2,400	~4,800	~1,200
K_i (nM)	<0.2	1.5	500

Supplementary Figure S4. Predicted complexation energy calculated using the using the eMBrAcE protocol.

The protocol optimizes the receptor, the ligand, and the receptor-ligand complex separately using a limited conformer search and the OPLS-AA force field. For the receptor, not all of the atoms are minimized: a 7Å shell of the receptor around the ligand was fully optimized, atoms 10Å away from the ligand is subjected to a constrained optimization with a force constant of 200, and all other atoms were not allowed to move. Initial positions of the ligand in the HDAC2 receptor (4LXZ pdb structure) and HDAC3 receptor (4A69 pdb structure) were determined using the Glide program in Schrodinger Suite 2013 in the HDAC2 (3MAX) structure. The complexation energies are given below and agree well with a linear fit to experimental log IC50.

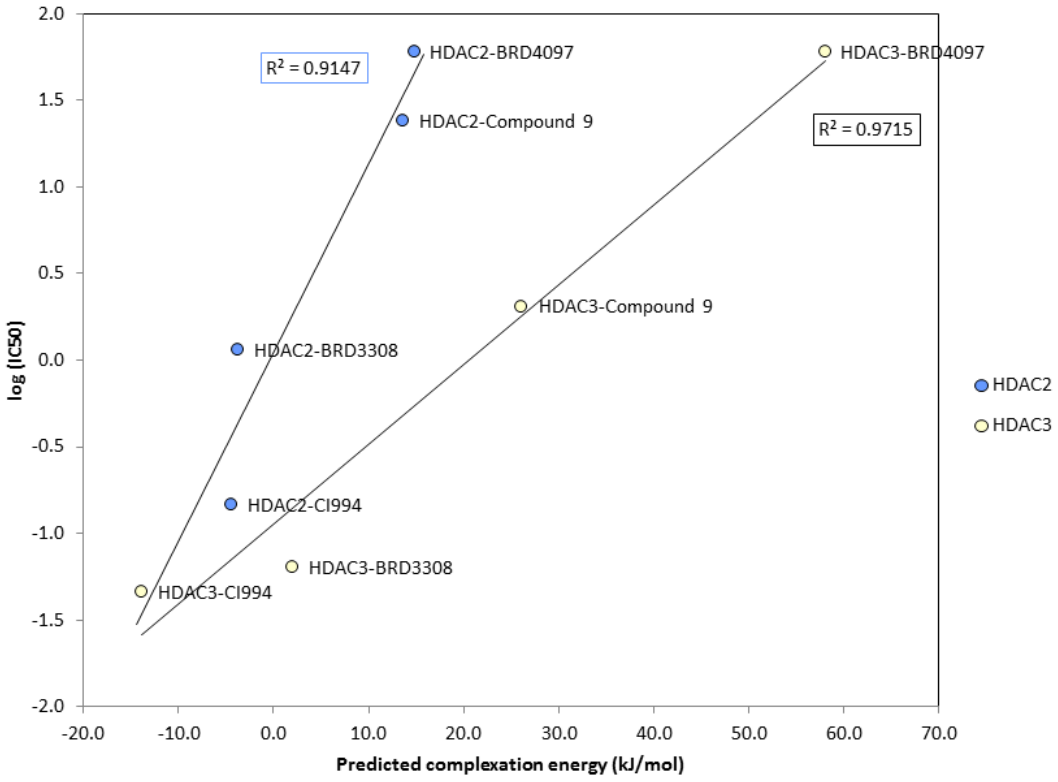

Supplementary Figure S5. Simulated kinetic selectivity for CI-994 and BRD3308 at 10 mg/kg i.p. dose in mouse.

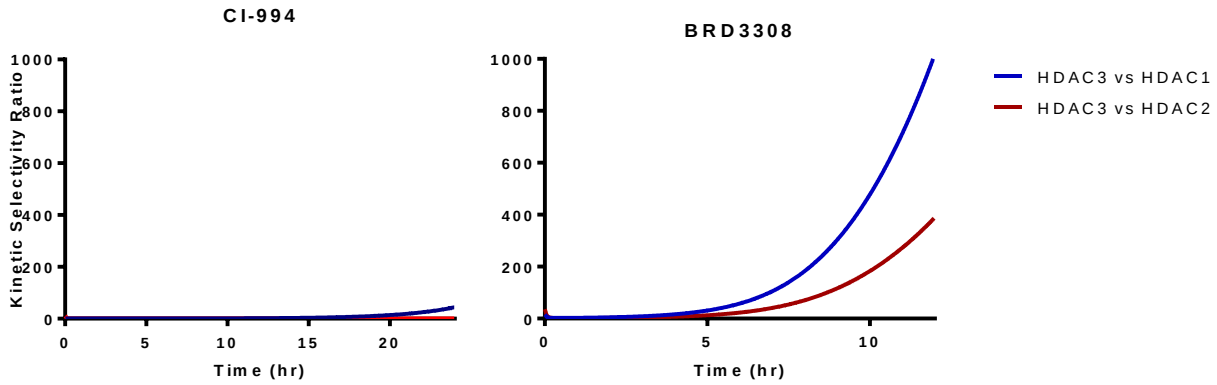

Supplementary Figure S6. Simulated target engagement profiles for HDAC 1, 2 and 3 in plasma for BRD3308 at 1 mg/kg dose i.p. (extrapolated).

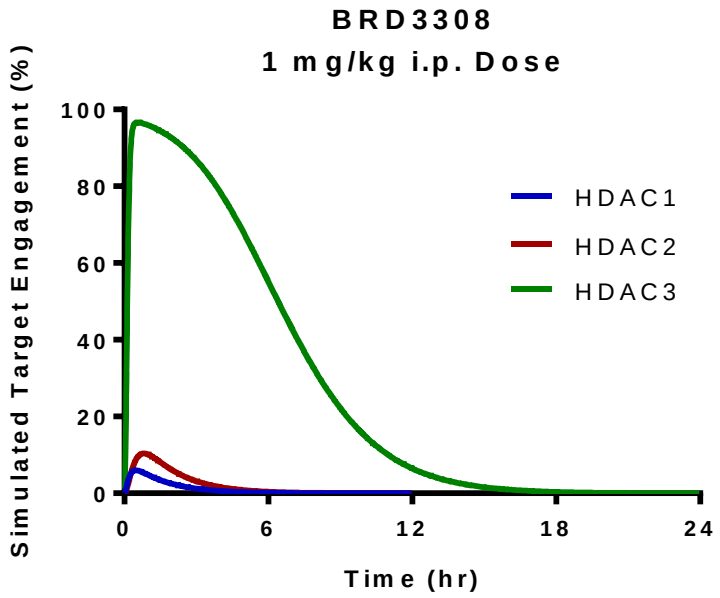

Supplementary Figure S7.

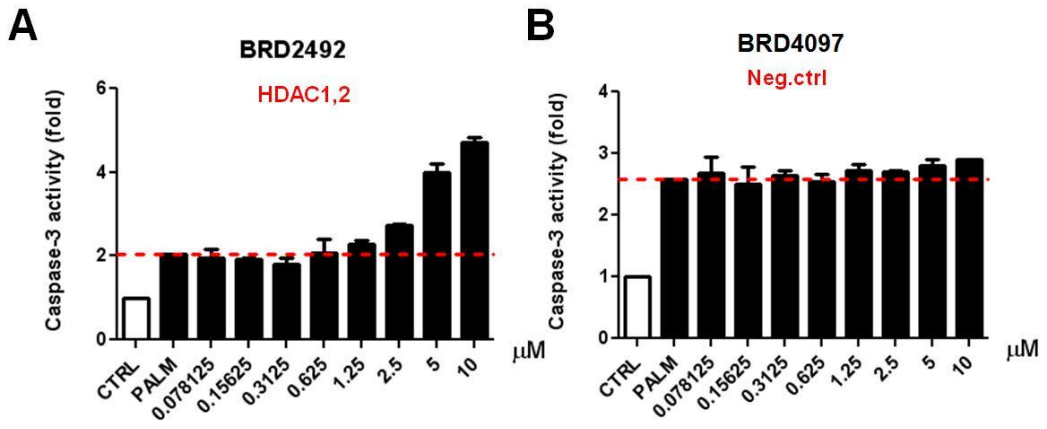

Tool kit compounds that do not inhibit HDAC3 do not suppress beta-cell apoptosis, as measured by caspase-3 activity. INS-1E cells were exposed to 0.5 mM palmitate (PALM) and the indicated compound (or vehicle, "CTRL") for 48 h. Apoptosis was measured by caspase-3 activity. Data (replicates of each concentration) were normalized to CTRL. Indicated HDAC targets listed in red.

Supplementary Figure S8.

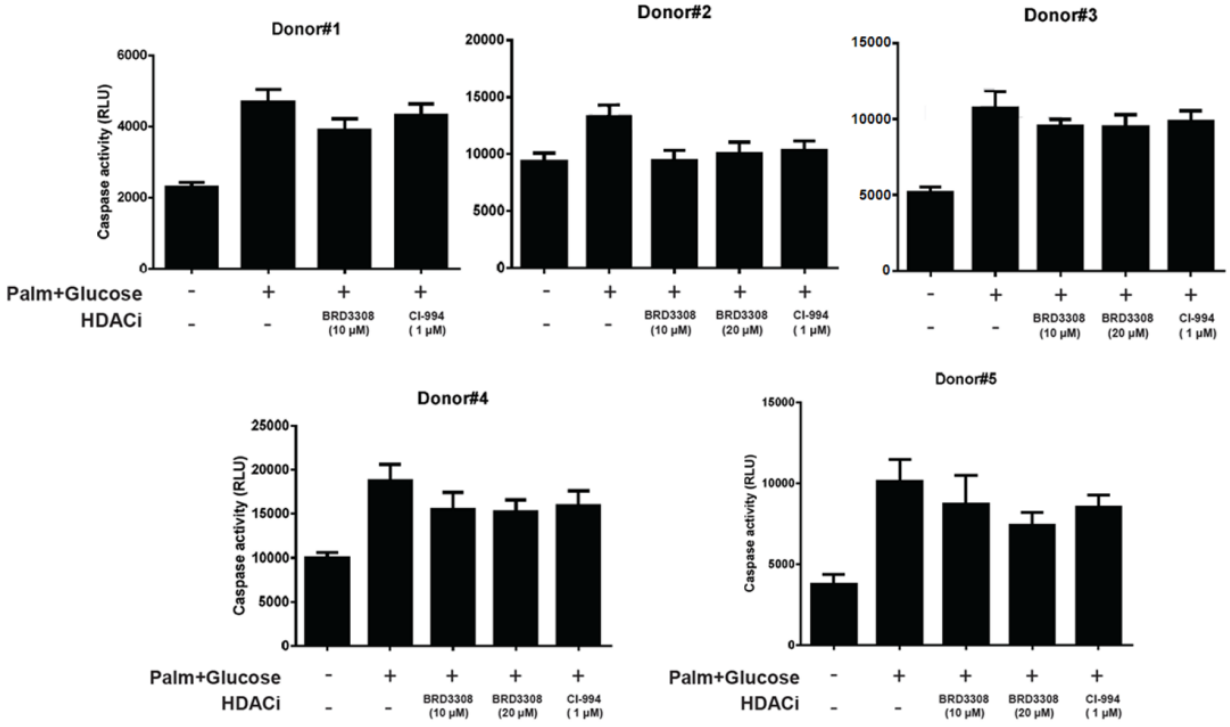

Chemical inhibition of HDAC3 prevents glucolipotoxicity-induced apoptosis in human islets – individual experiments. Dispersed human islets were exposed to 0.5 mM palmitate and 25 mM glucose (GLT) or vehicle and treated with either CI-994, BRD3308, or vehicle for 72 hours. Apoptosis was measured by caspase-3 activity assay. Data are presented as caspase-3 activity measured in RLU units from the five individual human donors, six replicates + SEM.

Supplementary Figure S9.

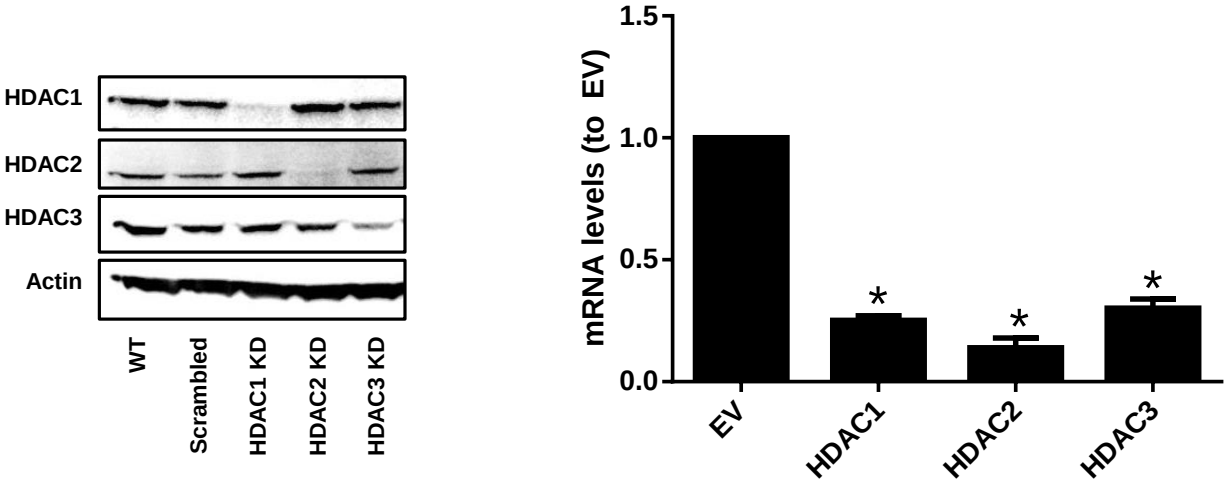

Confirmation of knock-down for each HDAC isoform in INS-1E cells (left, corresponding to Fig. 4a-c; right, corresponding to Fig. 4d).

Supplementary Figure S10.

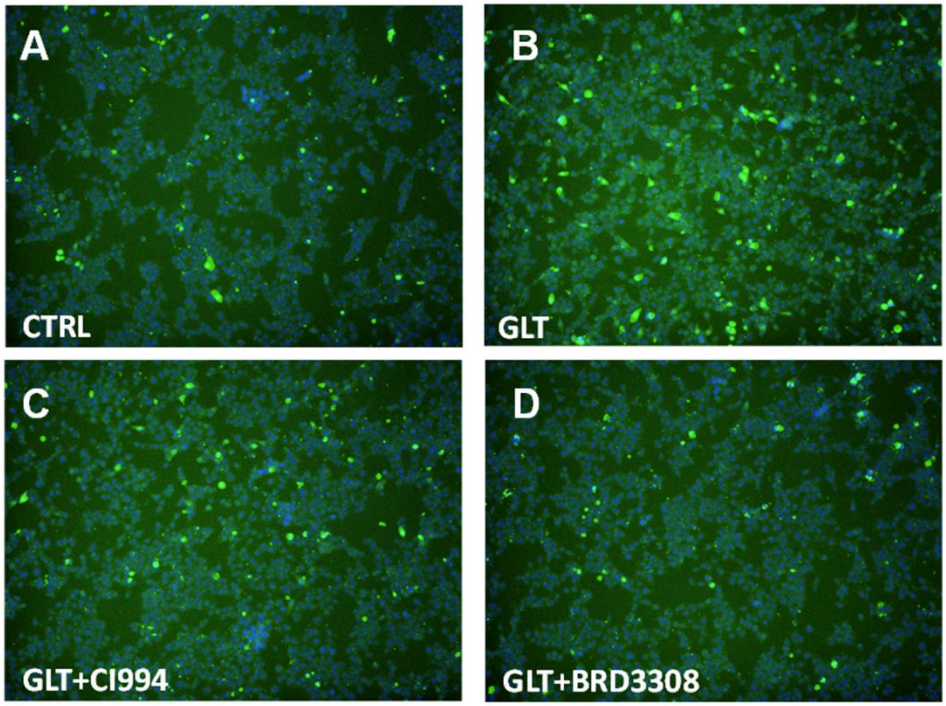

HDAC inhibition reduces palmitate and high glucose-induced ROS formation. INS-1E cells were exposed to 0.5 mM palmitate and 25 mM glucose (GLT) or vehicle and treated with BRD-3308 (10 μM), CI-994 (1μM) or vehicle for 48 hours. ROS was detected using the CM-H2DCFDA probe.

Supplementary Figure S11.

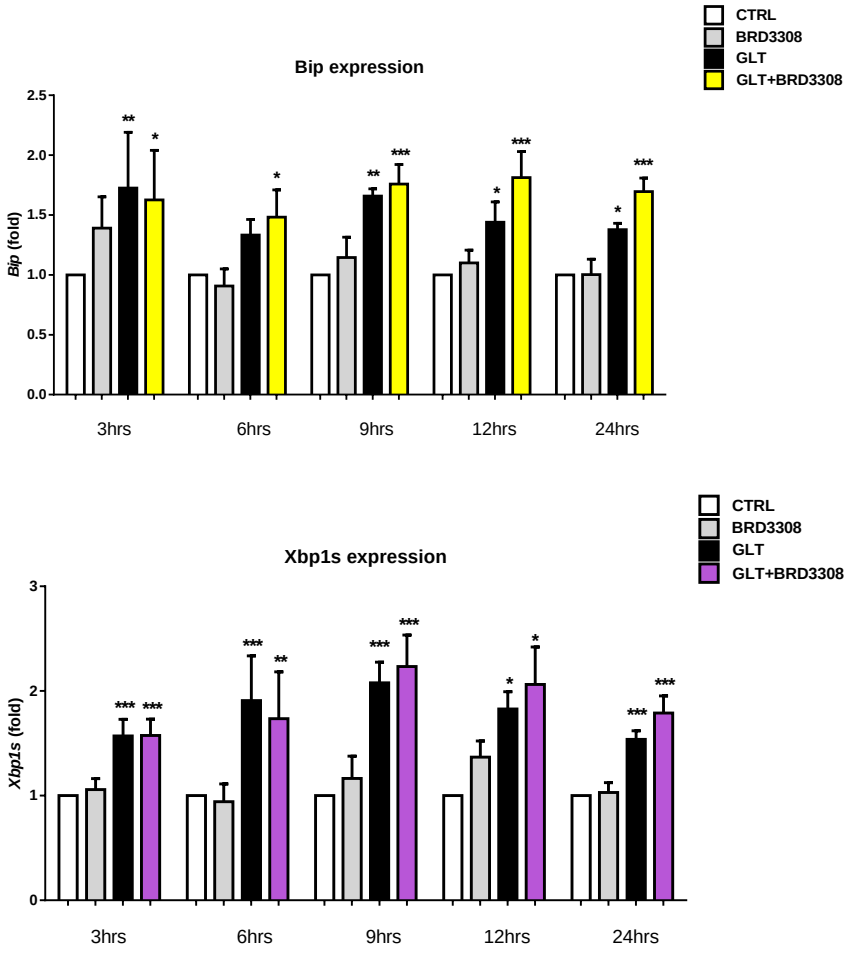

BRD3308 has no effect on Bip or Xbp1s expression in response to GLT. INS-1E cells were incubated in the absence or presence of 0.5 mM palmitate and 25mM glucose or vehicle, and treated with BRD3308 (10 μM) or DMSO for the indicated times. Gene expression was analyzed by qPCR. * $p<0.05$, ** $p<0.01$, *** $p<0.001$ vs. CTRL, ANOVA with Tukey-corrected tests.

Supplementary Figure S12.

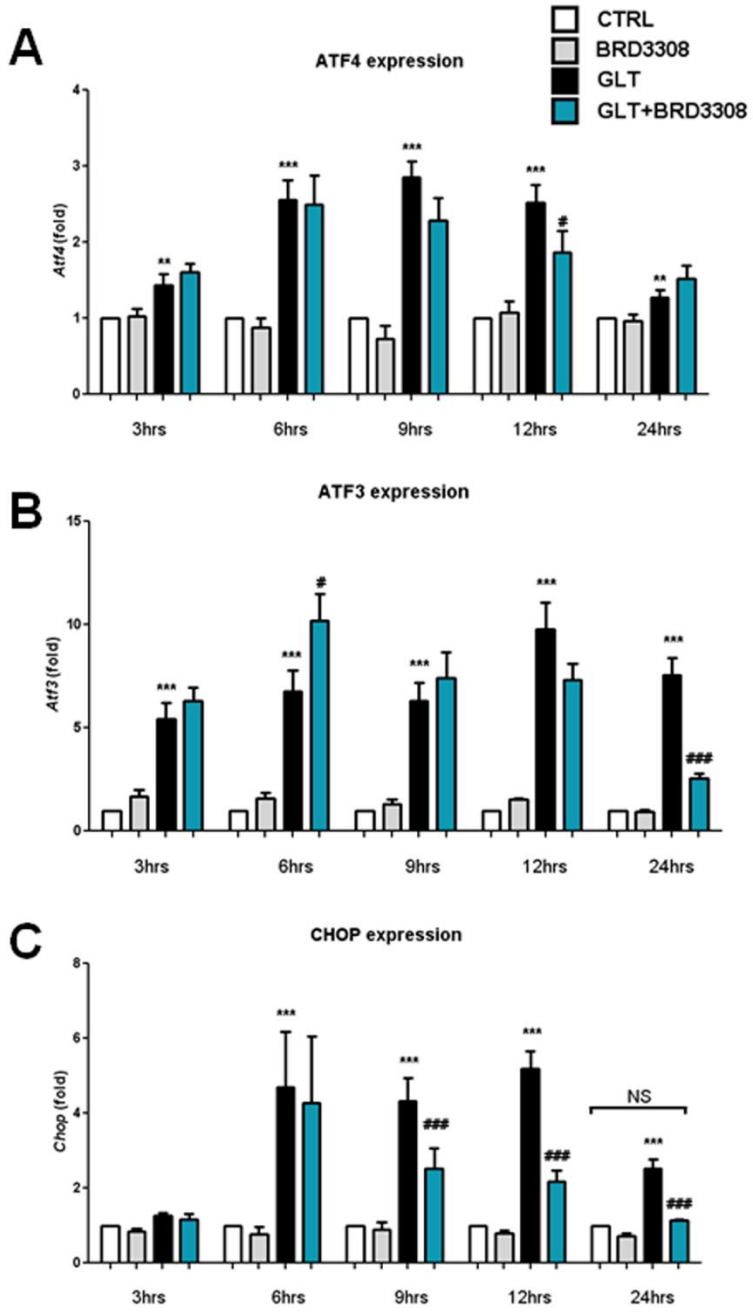

BRD3308 reduces Atf3 and Chop expression in response to GLT. INS-1E cells were incubated in the absence or presence of 0.5 mM palmitate and 25mM glucose, and treated with BRD3308 (10 μM) or DMSO for the indicated times. Gene expression was analyzed by qPCR. * p<0.05, ** p<0.01, *** p<0.001 vs. CTRL, # p<0.05, ### p<0.001 vs. respective treatment. ANOVA with Tukey -corrected tests.

Supplementary Figure S13.

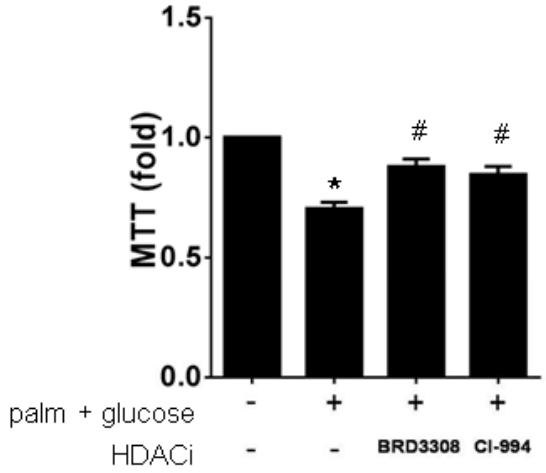

Inhibition of HDAC3 increases mitochondrial activity in glucolipotoxicity. INS-1E cells were exposed to 0.5 mM palmitate and 25mM glucose or vehicle and treated with CI-994 (1 μM), BRD3308 (10 μM) or vehicle for 3, 6, 9, 12, 24 or 48 h. Mitochondrial activity (48hrs) was measured by the MTT assay. * $p < 0.05$, with respect to untreated condition; # $p<0.05$, with respect to palmitate+glucose. ANOVA with Tukey -corrected tests.

Supplementary Figure S14. Primer sequences for qPCR experiments

primer sequences for qPCR experiments

Target	Forward	Reverse
β-actin	CACCCGCGAGTACAACCTTC	CCCATACCCACCATCACACC
Chop	CAGCGACAGAGCCAAAATAAC	TGTGGTGGTGTATGAAGATGC
Atf3	GGAGTCAGTCACCATCAACAA	CGCCTCCTTTTTCTCTCATCT
Bip	CGTATTTGGGAAAGAAGGTCA	CTTCTCTCCCTCTCTCTTATCCA
Ins1	GTCCTCTGGGAGCCCAAG	ACAGAGCCTCCACCAGG
Ins2	ATCCTCTGGGAGCCCCGC	AGAGAGCTTCCACCAAG
ATtf4	GTTGGTCAGTGCCTCAGACA	CATTCGAAACAGAGCATCGA
Xbp1s	GAGTCCGCAGCAGGTG	GCGTCAGAATCCATGGGA
IκBα	TCCTCAACTTCCAGAACAACC	GCAAGATGGAGAGGGGTATTT

Compound Characterization Material

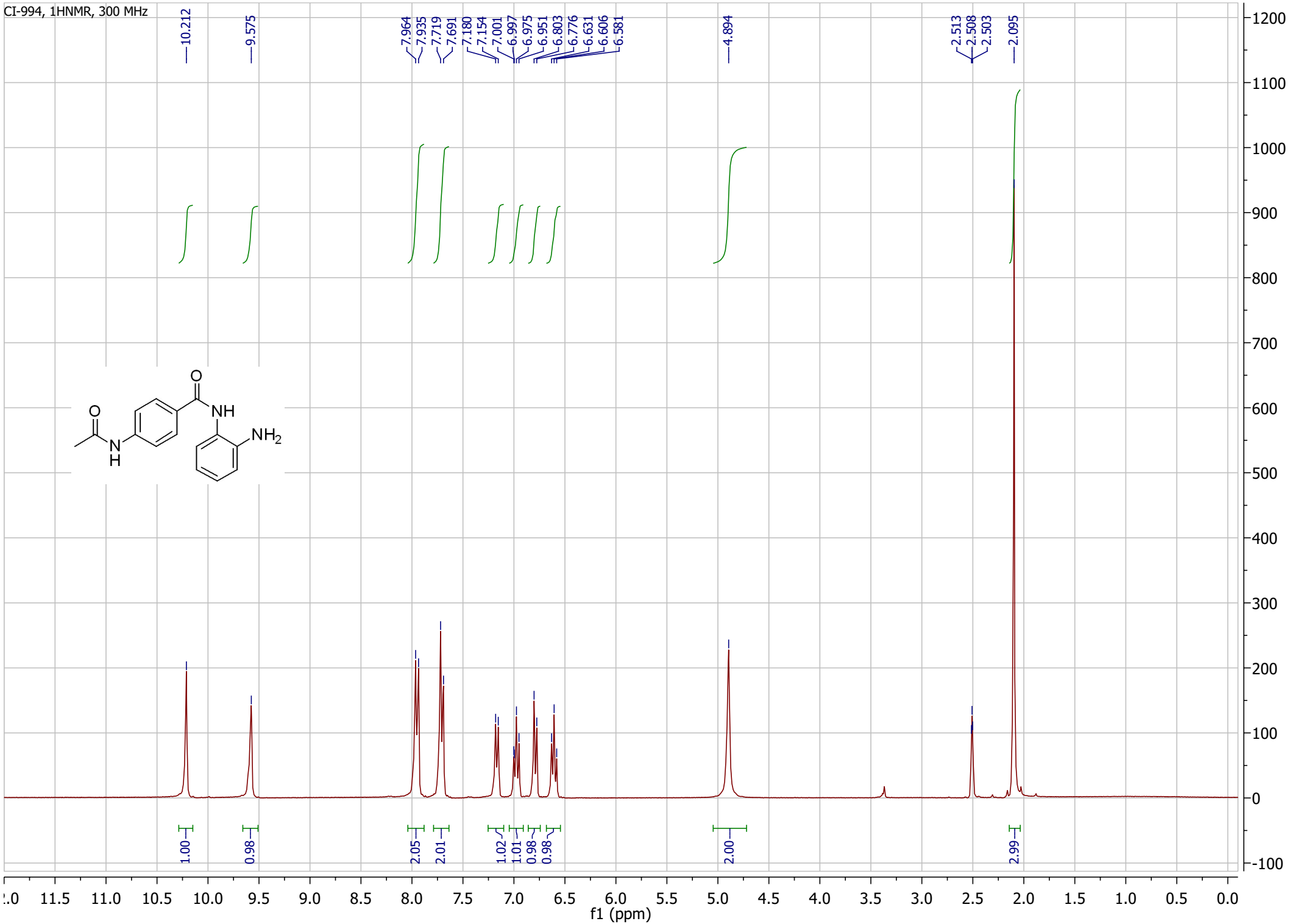
CI-994, 1HNMR, 300 MHz
10.212
9.575
7.964
7.935
7.719
7.691
7.180
7.154
7.001
6.997
6.975
6.951
6.803
6.776
6.631
6.606
6.581
4.894
2.513
2.508
2.503
2.095
1.00
0.98
2.05
2.01
1.02
1.01
0.98
0.98
2.00
2.99
f1 (ppm)

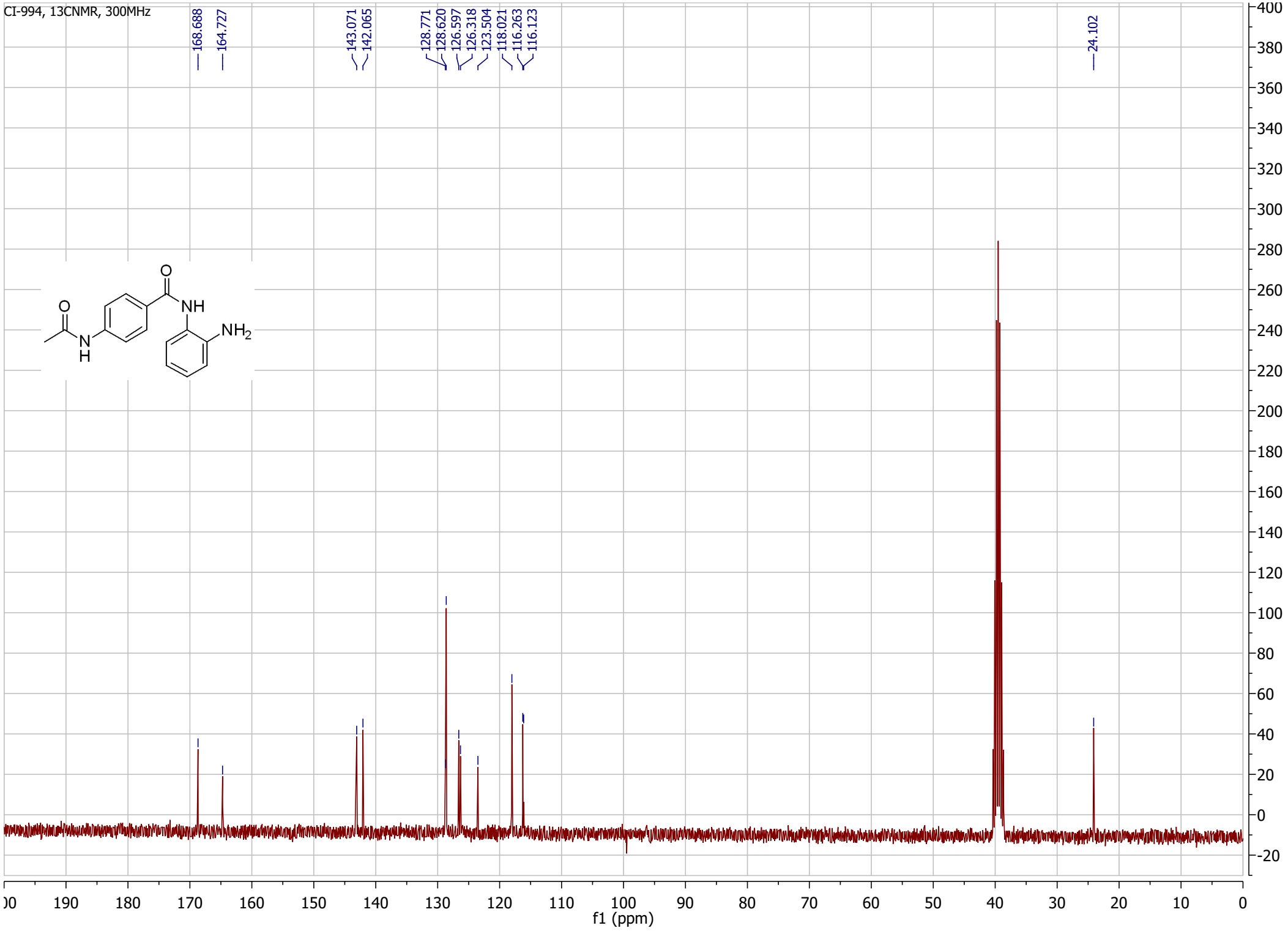
CI-994, 13CNMR, 300MHz
168.688
164.727
143.071
142.065
128.771
128.620
126.597
126.318
123.504
118.021
116.263
116.123
24.102
O
NH
NH2
O
N
H
f1 (ppm)

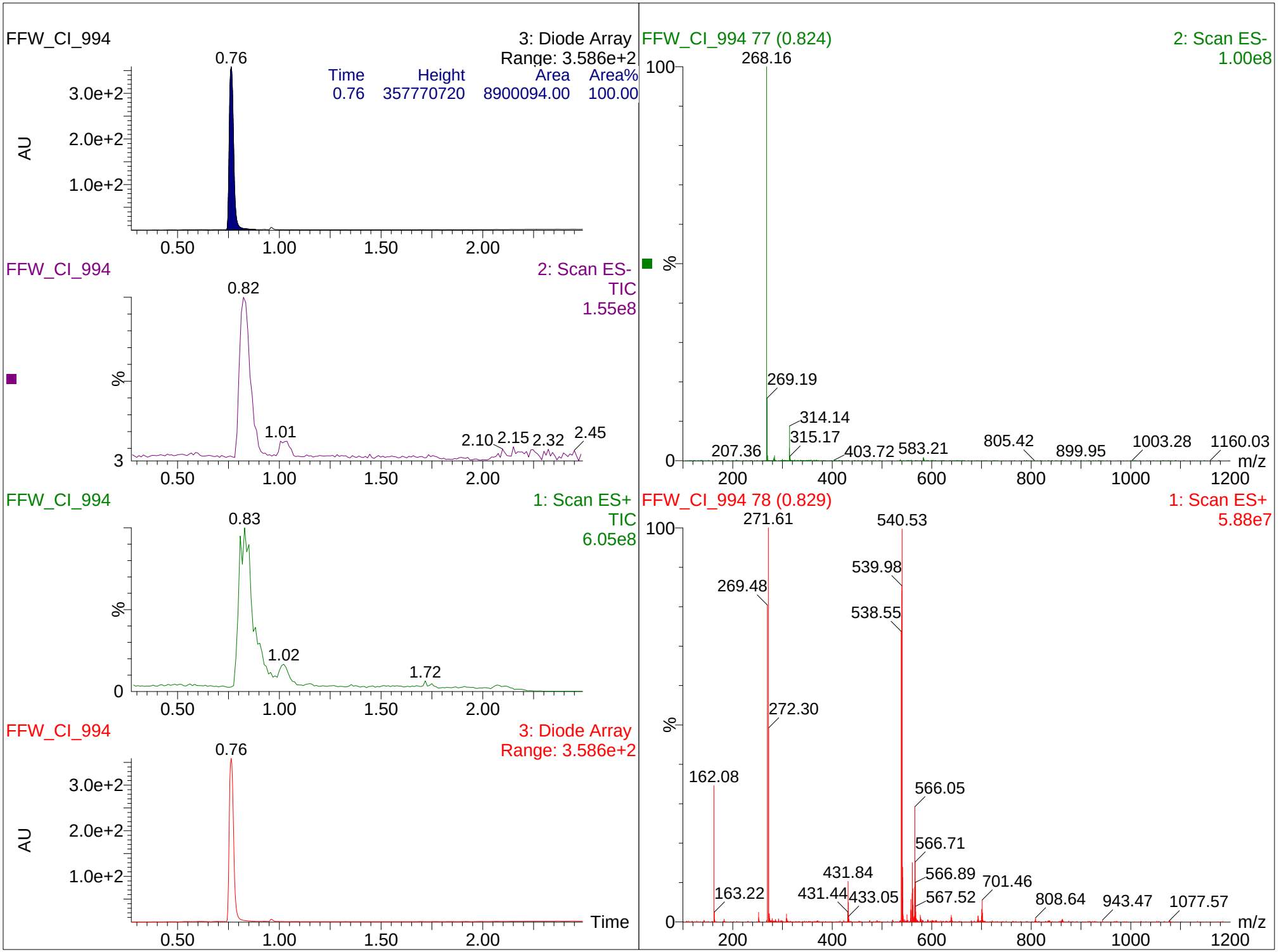
FFW_CI_994
3: Diode Array
Range: 3.586e+2
Time Height Area Area%
0.76 357770720 8900094.00 100.00
0.76
AU
3.0e+2
2.0e+2
1.0e+2
0.50 1.00 1.50 2.00
FFW_CI_994
2: Scan ES-
TIC
1.55e8
0.82
1.01
2.10 2.15 2.32 2.45
%
3
FFW_CI_994
1: Scan ES+
TIC
6.05e8
0.83
1.02
1.72
%
0
FFW_CI_994
3: Diode Array
Range: 3.586e+2
0.76
AU
Time
FFW_CI_994 77 (0.824)
2: Scan ES-
1.00e8
268.16
269.19
314.14
315.17
207.36
403.72 583.21
805.42
899.95
1003.28
1160.03
100
%
0
200 400 600 800 1000 1200
m/z
FFW_CI_994 78 (0.829)
1: Scan ES+
5.88e7
271.61
540.53
539.98
269.48
538.55
272.30
162.08
566.05
566.71
431.84
566.89
701.46
163.22
431.44
433.05
567.52
808.64
943.47
1077.57
100
%
0
200 400 600 800 1000 1200
m/z

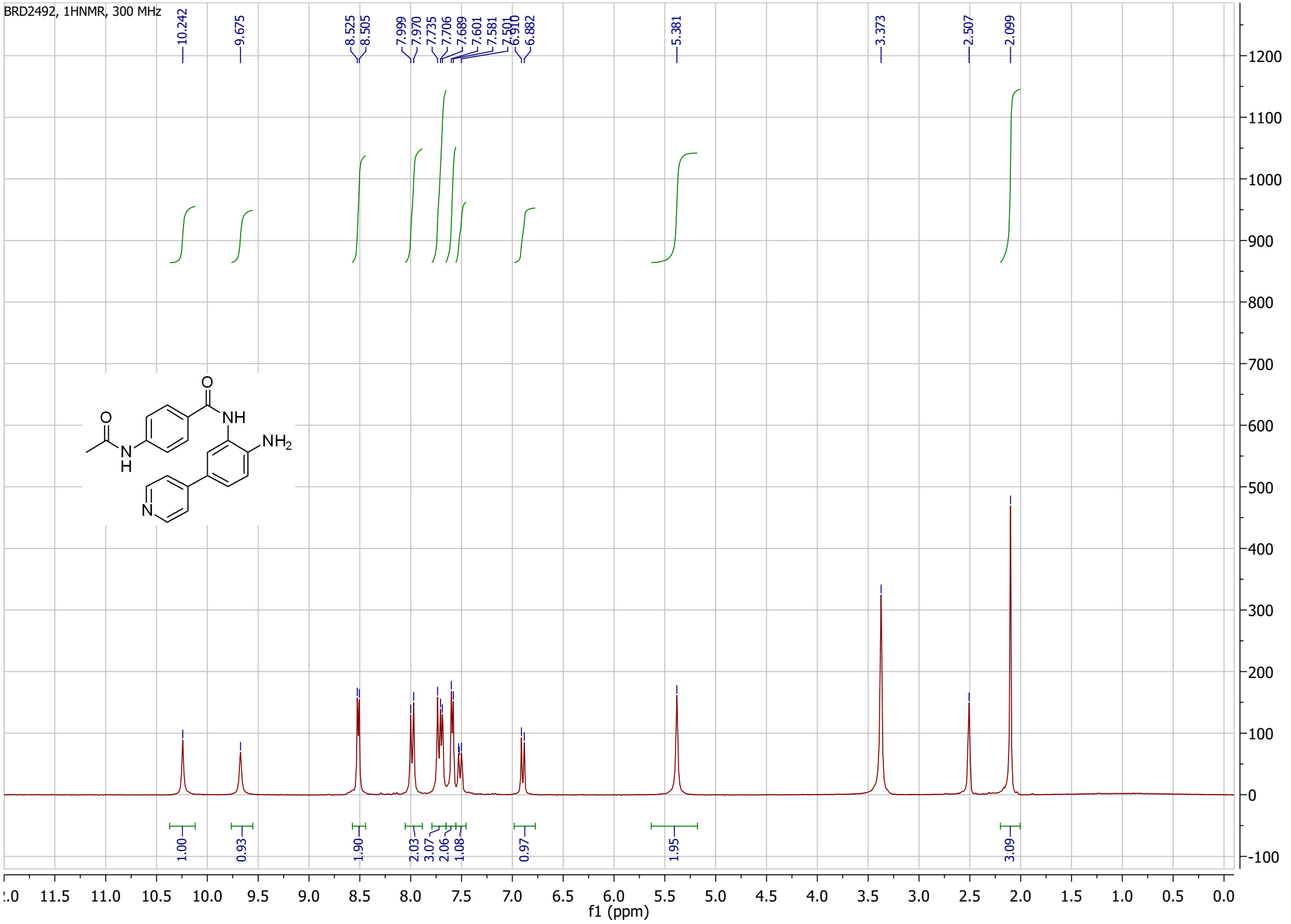
BRD2492, 1HNMR, 300 MHz
10.242
9.675
8.525
8.505
7.999
7.970
7.735
7.706
7.689
7.601
7.581
7.501
6.910
6.882
5.381
3.373
2.507
2.099
O
NH
NH2
O
N
H
N
1.00
0.93
1.90
2.03
3.07
2.06
1.08
0.97
1.95
3.09
f1 (ppm)

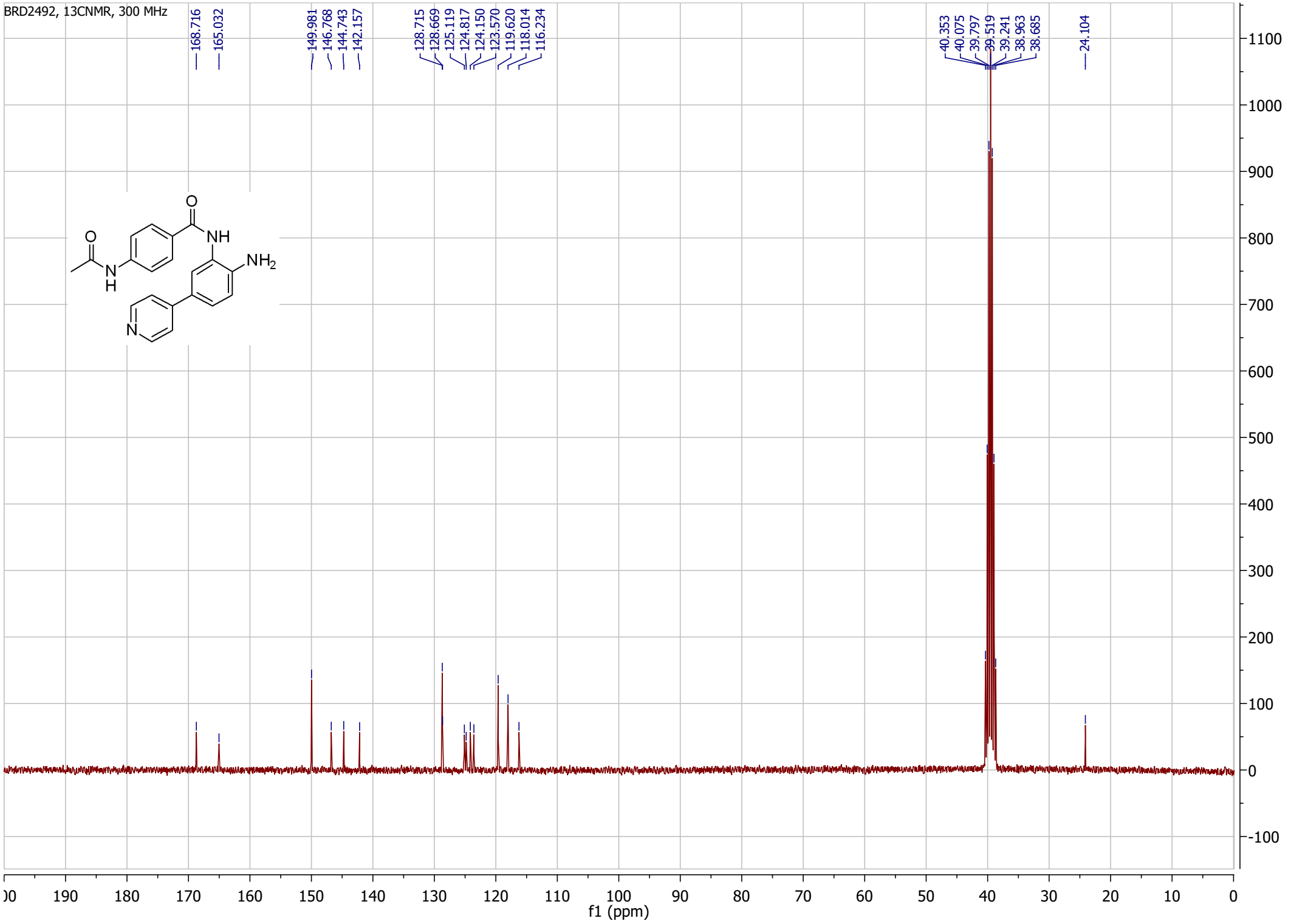
BRD2492, 13CNMR, 300 MHz
168.716
165.032
149.981
146.768
144.743
142.157
128.715
128.669
125.119
124.817
124.150
123.570
119.620
118.014
116.234
40.353
40.075
39.797
39.519
39.241
38.963
38.685
24.104
O
NH
NH2
O
N
H
N
f1 (ppm)

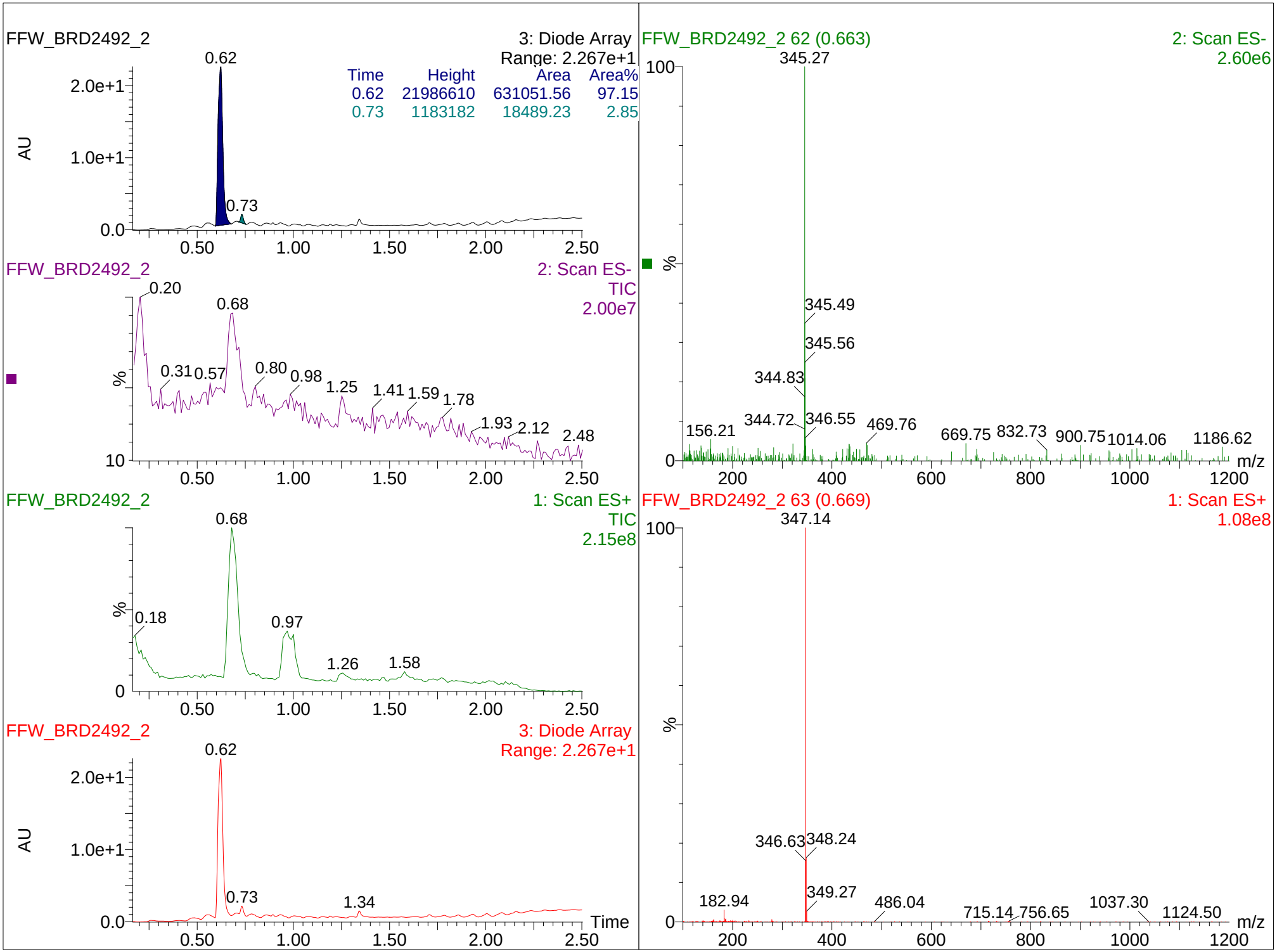
FFW_BRD2492_2
3: Diode Array
Range: 2.267e+1
Time Height Area Area%
0.62 21986610 631051.56 97.15
0.73 1183182 18489.23 2.85
AU
0.62
0.73
FFW_BRD2492_2
2: Scan ES-
TIC
2.00e7
%
0.20
0.68
0.31
0.57
0.80
0.98
1.25
1.41
1.59
1.78
1.93
2.12
2.48
FFW_BRD2492_2
1: Scan ES+
TIC
2.15e8
%
0.68
0.18
0.97
1.26
1.58
FFW_BRD2492_2
3: Diode Array
Range: 2.267e+1
AU
0.62
0.73
1.34
Time
FFW_BRD2492_2 62 (0.663)
2: Scan ES-
2.60e6
%
345.27
345.49
345.56
344.83
344.72
346.55
156.21
469.76
669.75
832.73
900.75
1014.06
1186.62
m/z
FFW_BRD2492_2 63 (0.669)
1: Scan ES+
1.08e8
%
347.14
346.63
348.24
349.27
182.94
486.04
715.14
756.65
1037.30
1124.50
m/z

SBF-8002-053 in DMSO-D6
File.No.B151208A20

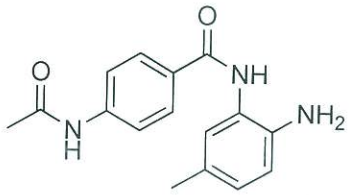

SAMPLE INFORMATION

Sample Name:	**SBF-8002-053 # IP0812416**	Acquired By:	System
Sample Type:	Unknown	Sample Set Name:	121208_01
Vial:	1:B,7	Acq. Method Set:	PDA_METH_1A
Injection #:	1	Proc. Chnl. Descr.:	**PDA 254.0 nm**
Injection Volume:	1.80 ul	Date Acquired:	12/12/2008 7:40:22 PM IST
Run Time:	6.0 Minutes	Date Processed:	12/12/2008 8:27:01 PM IST
Project Name:	DEC_08		

Column:ACQUITY BEH C-18 (2.1 x50mm,1.7u)
Column Temp:25°C
Mobile Phase:A:Acetonitrile
MobilePhase:B:5mM NH4OAc
Flow:0.5ml/min
Gradient programe:
T/%B:0.01/90,0.5/90,3/10,6/10,
Diluent: ACN:WATER (1:1)

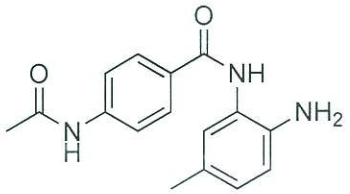

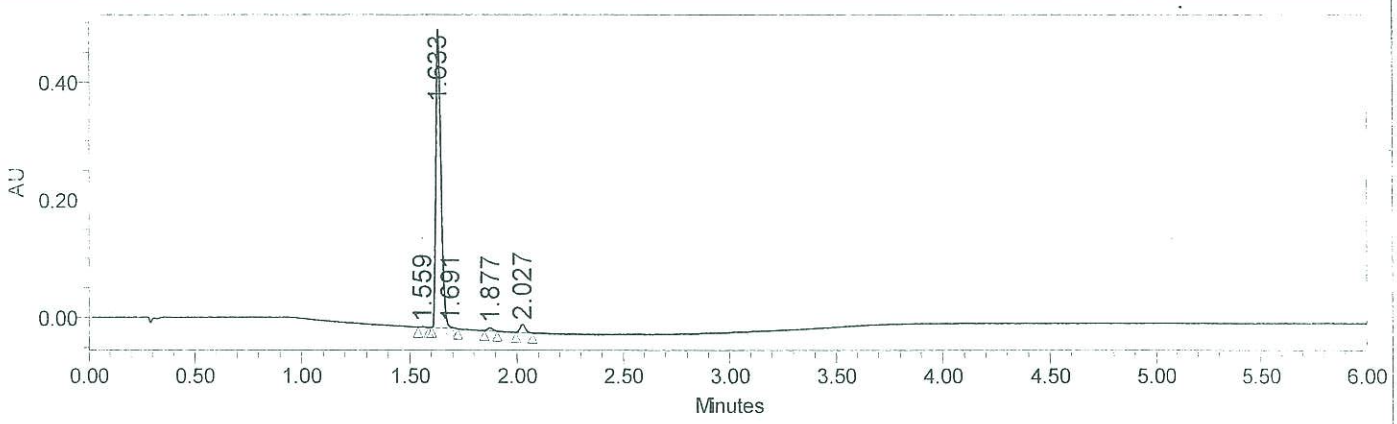

	RT	Area	% Area
1	1.56	1582	0.18
2	1.63	828644	95.87
3	1.69	2638	0.31
4	1.88	8657	1.00
5	2.03	22834	2.64

12/12/2008

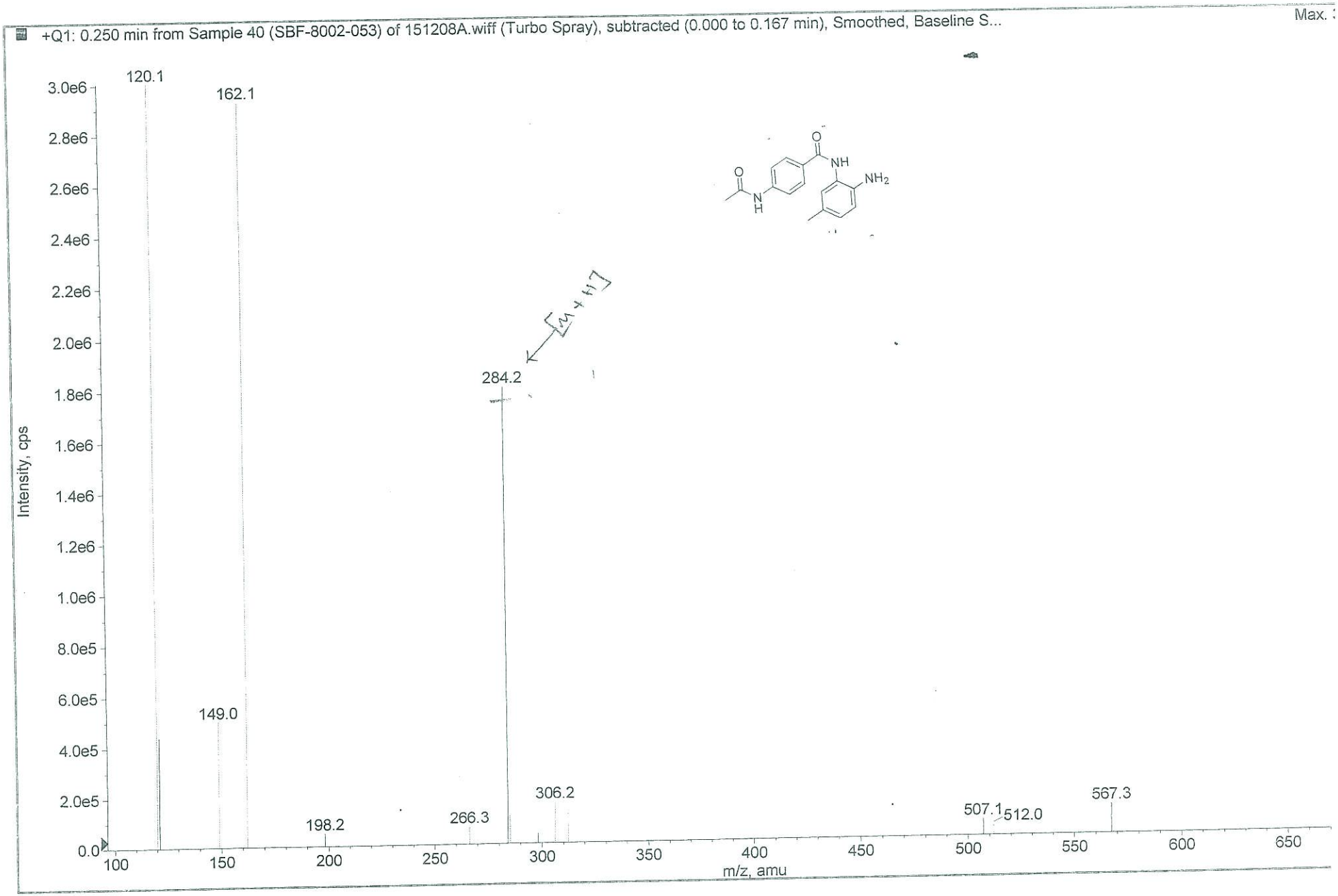
+Q1: 0.250 min from Sample 40 (SBF-8002-053) of 151208A.wiff (Turbo Spray), subtracted (0.000 to 0.167 min), Smoothed, Baseline S...
Max. :
Intensity, cps
m/z, amu
120.1
162.1
284.2
149.0
198.2
266.3
306.2
507.1
512.0
567.3
M + H
NH
NH2
O
N
H

SBF-MA1204-093 in DMSO-d6
File.No.101012B102

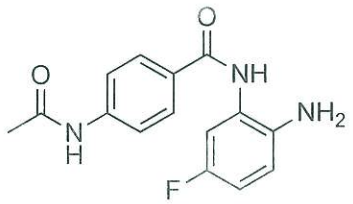

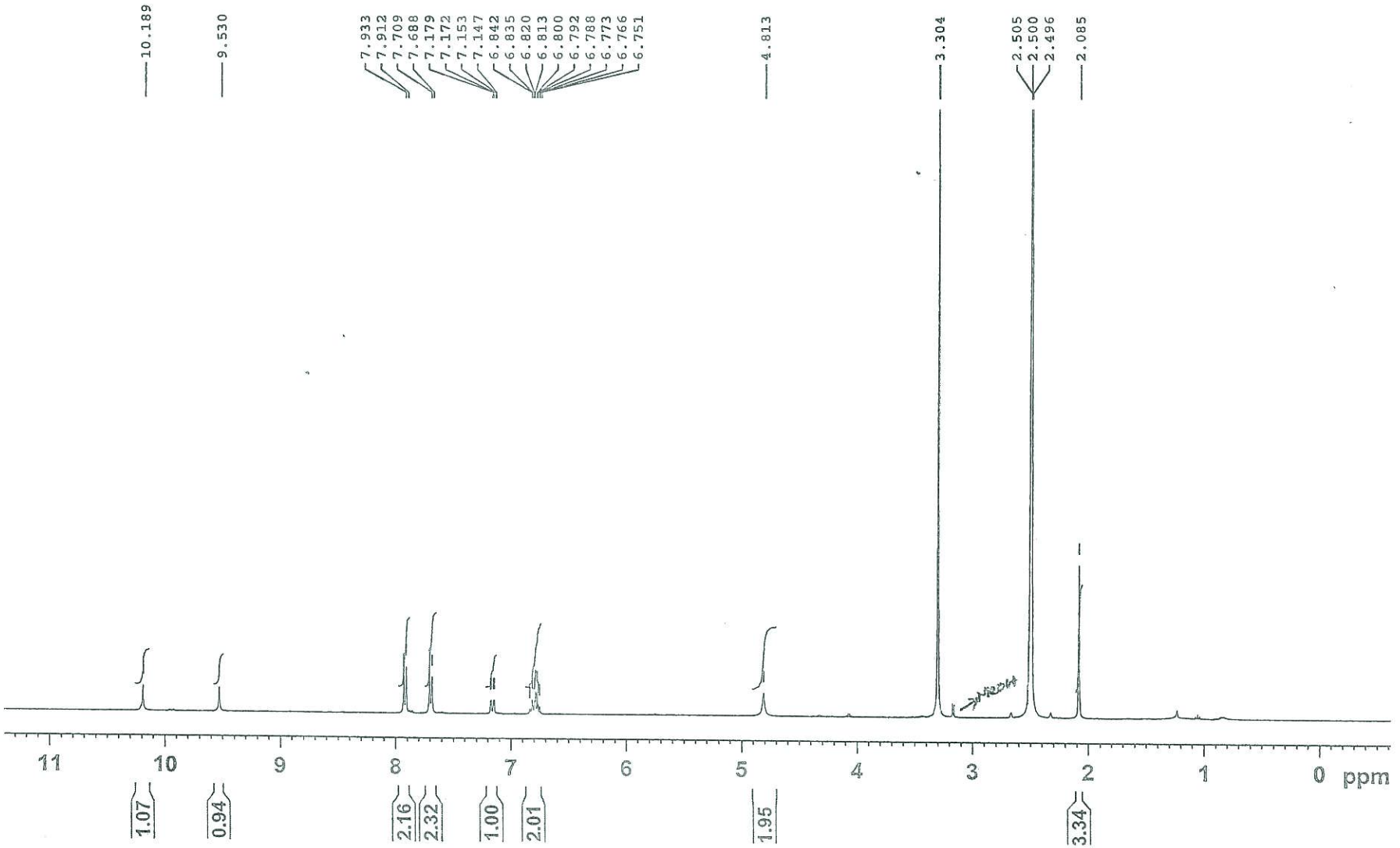

Sample Name: **SBF-MA1204-093 # IP12090381**
Sample Type: Unknown
Vial: 2:D,7
Injection #: 1
Injection Volume: 1.00 ul
Run Time: 6.0 Minutes
Project Name: SAPL_UNIT-2_AMCL_ALC-10-SEP-12

Acquired By: System
Sample Set Name: 120912_3
Acq. Method Set: PDA_METH_2A
Proc. Chnl. Descr.: **PDA 254.0 nm**
Date Acquired: 9/12/2012 7:04:44 PM IST

Column: Acquity UPLC BEH C-18 {2.1 x50mm,1.7u}
Column Temp:25℃
Mobile Phase:A: Acetonitrile
Mobile Phase:B:0.025% Aq TFA
Flow:0.5ml/min
Gradient programe:
T/%B:0.01/90,0.5/90,3/10,6/10
Diluent: ACN:Water

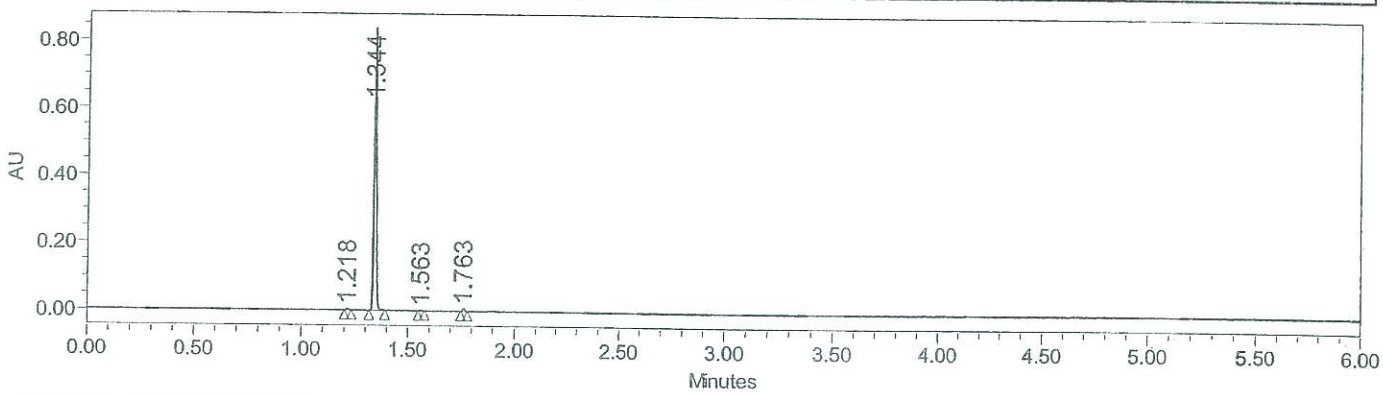

	RT	Area	% Area
1	1.22	4899	0.73
2	1.34	656479	98.25
3	1.56	975	0.15
4	1.76	5838	0.87

Sample Information

Sample Name	:SBF-MA1204-093
Date Acquired	: 9/15/2012 3:19:34 PM
Data File	: 150912M 34.lcd
Method File	: Test Method - LCMS.lcm
Tuning File	: D:\Shimadzu MS Data\Tuning Files\EI 090208.lct
Vial	:26

Column: X-Bridge C-18(50x3.0mm,3.5um)
Mobilephase A:0.05% TFA in Water , B:ACN(Gradient)
T%B:0.01/10,0.5/10,4/90,8/90
Flow:0.8mL/min;

Chromatogram

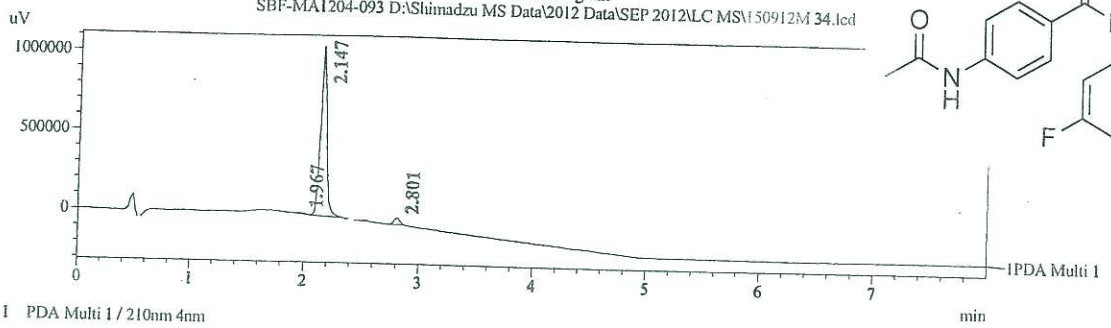

I PDA Multi 1 / 210nm 4nm

MS Spectrum

Ret Time:2.133-2.233
Polarity:Pos: Base Peak:288.05

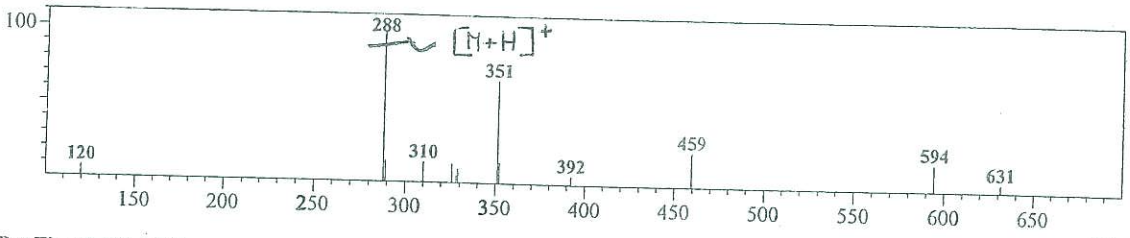

Ret Time:2.800-2.867
Polarity:Pos: Base Peak:227.20

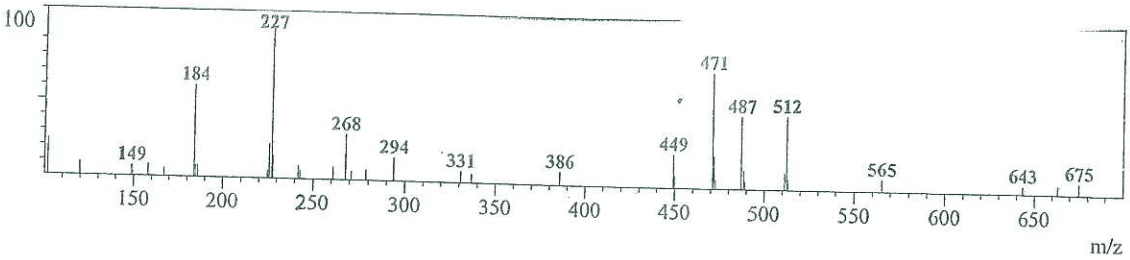

PeakTable

PDA Ch1 210nm 4nm

Peak#	Ret. Time	Area	Area %
1	1.967	18737	0.455
2	2.147	3964815	96.306
3	2.801	133351	3.239
Total		4116904	100.000

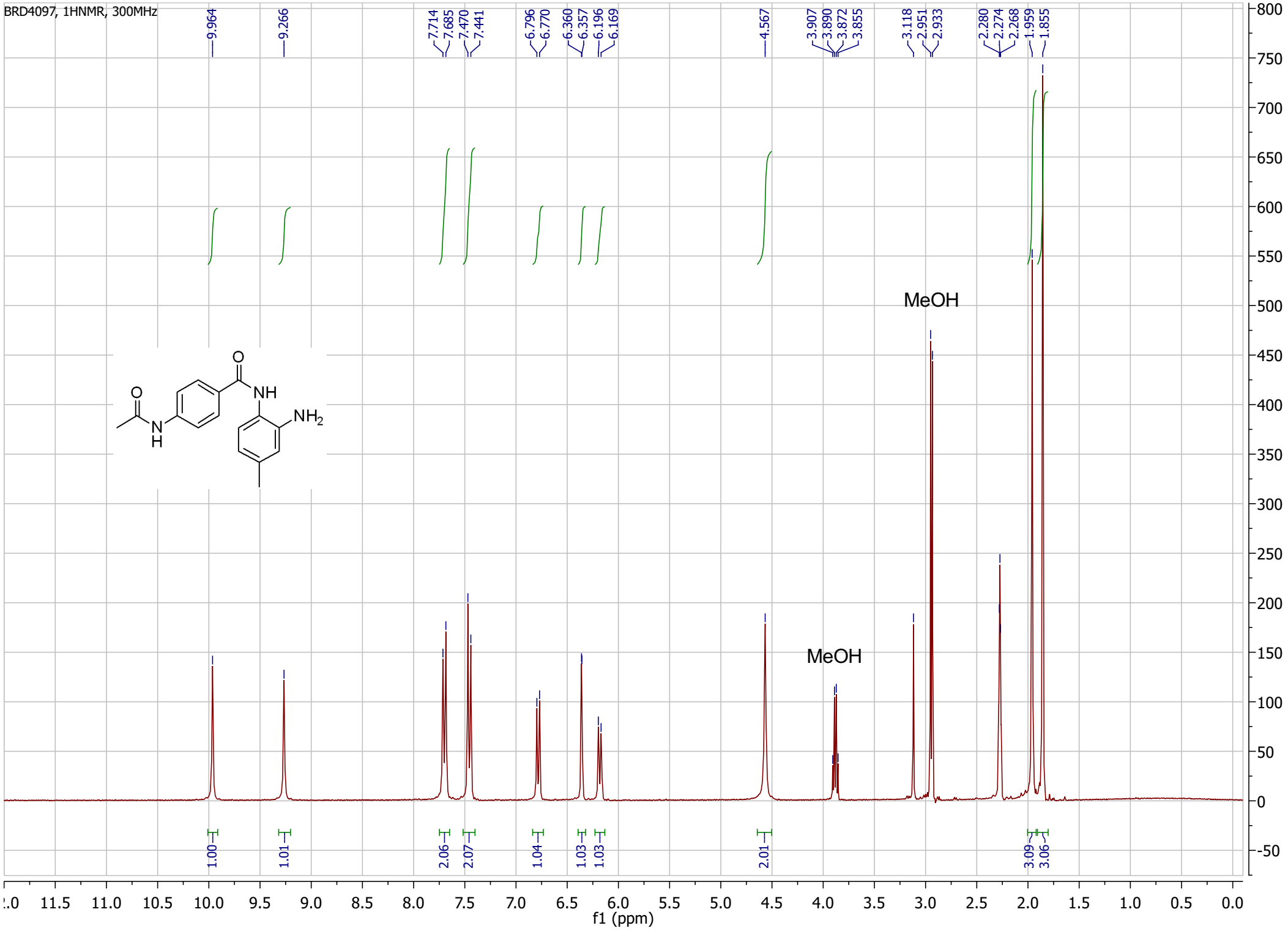
BRD4097, 1HNMR, 300MHz
9.964
9.266
7.714
7.685
7.470
7.441
6.796
6.770
6.360
6.357
6.196
6.169
4.567
3.907
3.890
3.872
3.855
3.118
2.951
2.933
2.280
2.274
2.268
1.959
1.855
MeOH
MeOH
O
NH
NH2
N
H
O
1.00
1.01
2.06
2.07
1.04
1.03
1.03
2.01
3.09
3.06
f1 (ppm)

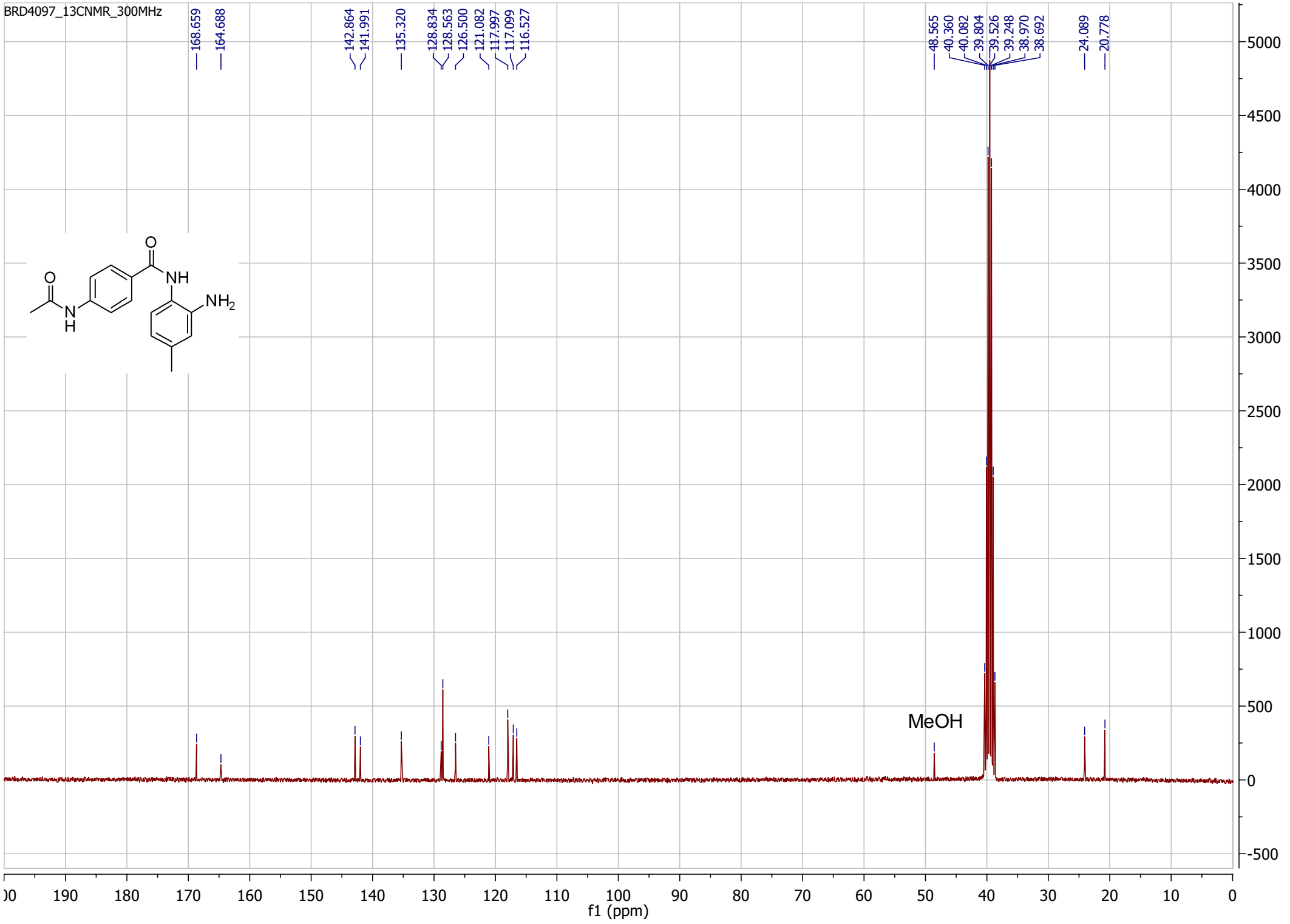
BRD4097_13CNMR_300MHz
168.659
164.688
142.864
141.991
135.320
128.834
128.563
126.500
121.082
117.997
117.099
116.527
48.565
40.360
40.082
39.804
39.526
39.248
38.970
38.692
24.089
20.778
MeOH
O
NH
NH2
N
H
O
5000
4500
4000
3500
3000
2500
2000
1500
1000
500
0
-500
190
180
170
160
150
140
130
120
110
100
90
80
70
60
50
40
30
20
10
0
f1 (ppm)

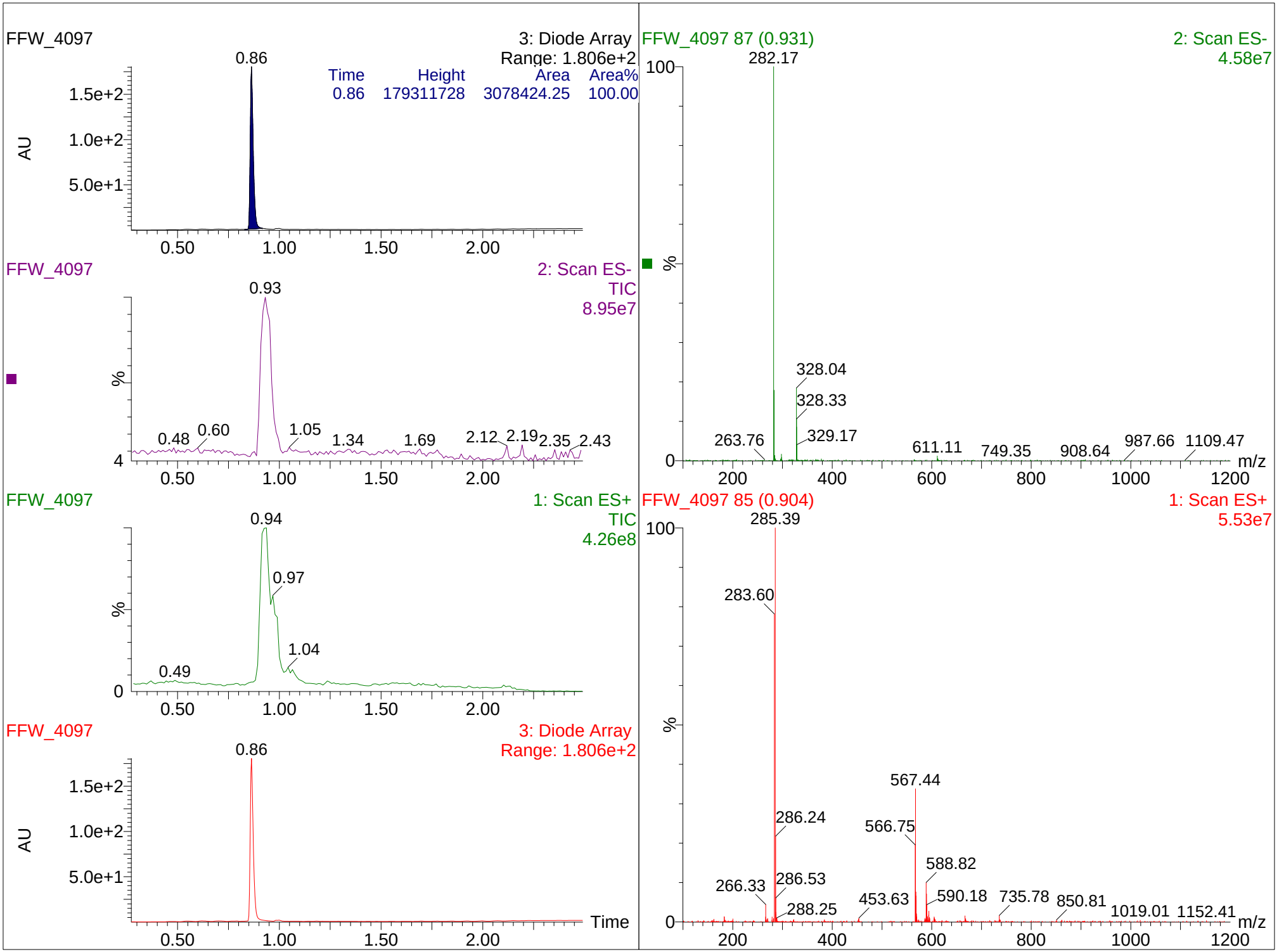
FFW_4097
3: Diode Array
Range: 1.806e+2
Time Height Area Area%
0.86 179311728 3078424.25 100.00
AU
FFW_4097
2: Scan ES-
TIC
8.95e7
FFW_4097
1: Scan ES+
TIC
4.26e8
FFW_4097
3: Diode Array
Range: 1.806e+2
Time
FFW_4097 87 (0.931)
2: Scan ES-
4.58e7
m/z
FFW_4097 85 (0.904)
1: Scan ES+
5.53e7
m/z

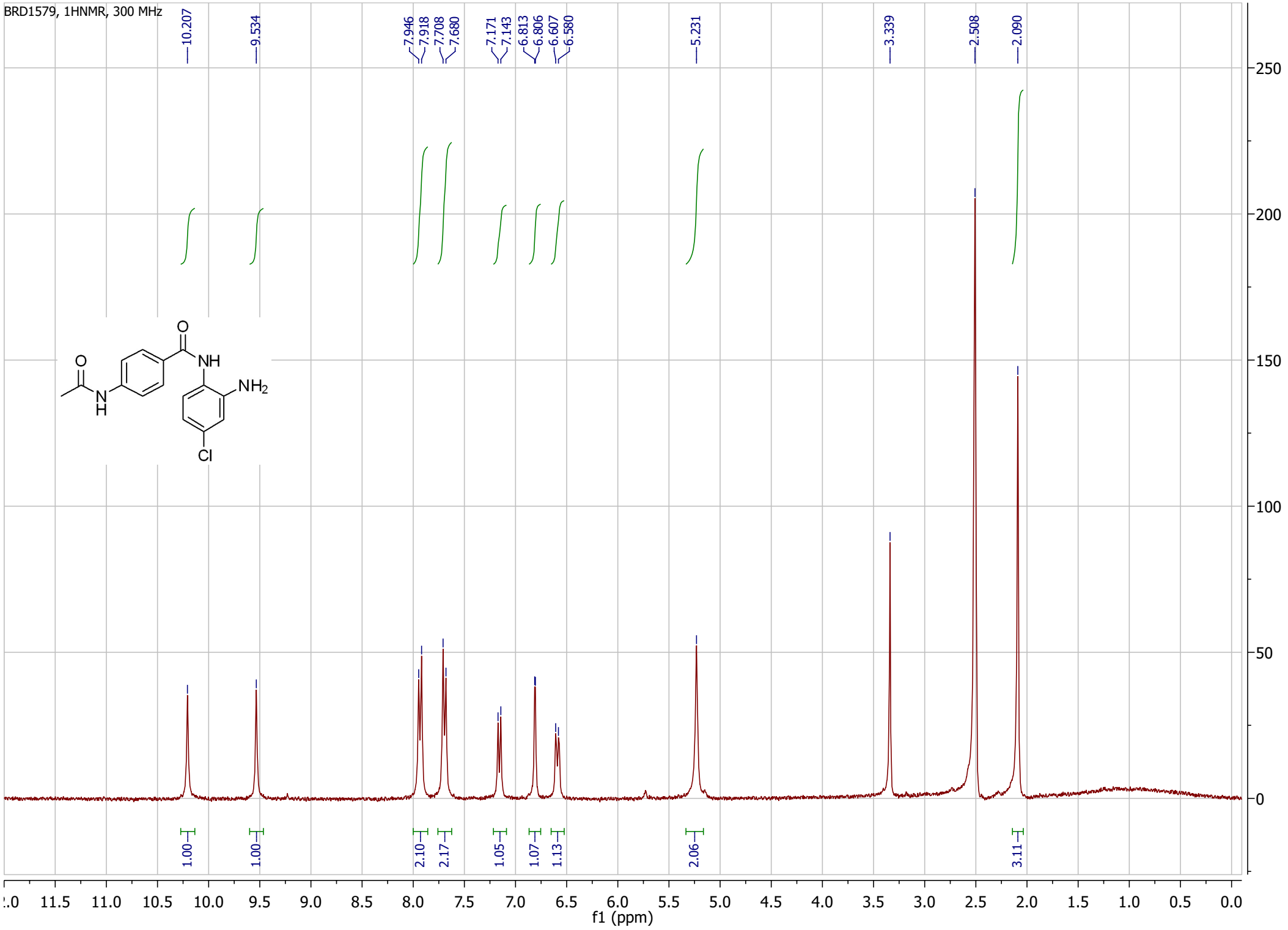
BRD1579, 1HNMR, 300 MHz
10.207
9.534
7.946
7.918
7.708
7.680
7.171
7.143
6.813
6.806
6.607
6.580
5.231
3.339
2.508
2.090
O
NH
NH2
O
N
H
Cl
1.00
1.00
2.10
2.17
1.05
1.07
1.13
2.06
3.11
250
200
150
100
50
0
f1 (ppm)

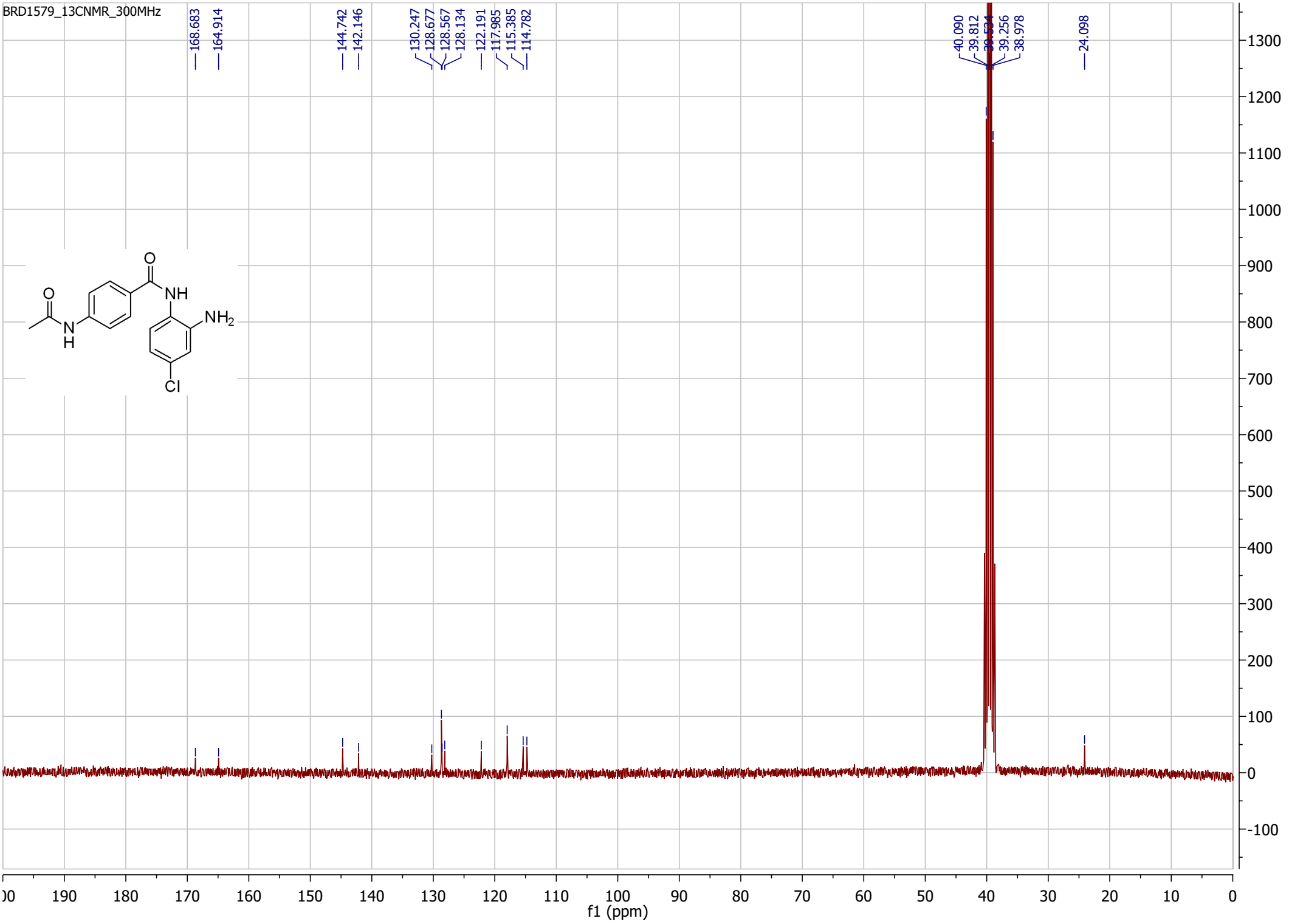
BRD1579_13CNMR_300MHz
168.683
164.914
144.742
142.146
130.247
128.677
128.567
128.134
122.191
117.985
115.385
114.782
40.090
39.812
39.534
39.256
38.978
24.098
O
NH
NH2
O
N
H
Cl
1300
1200
1100
1000
900
800
700
600
500
400
300
200
100
0
-100
190
180
170
160
150
140
130
120
110
100
90
80
70
60
50
40
30
20
10
0
f1 (ppm)

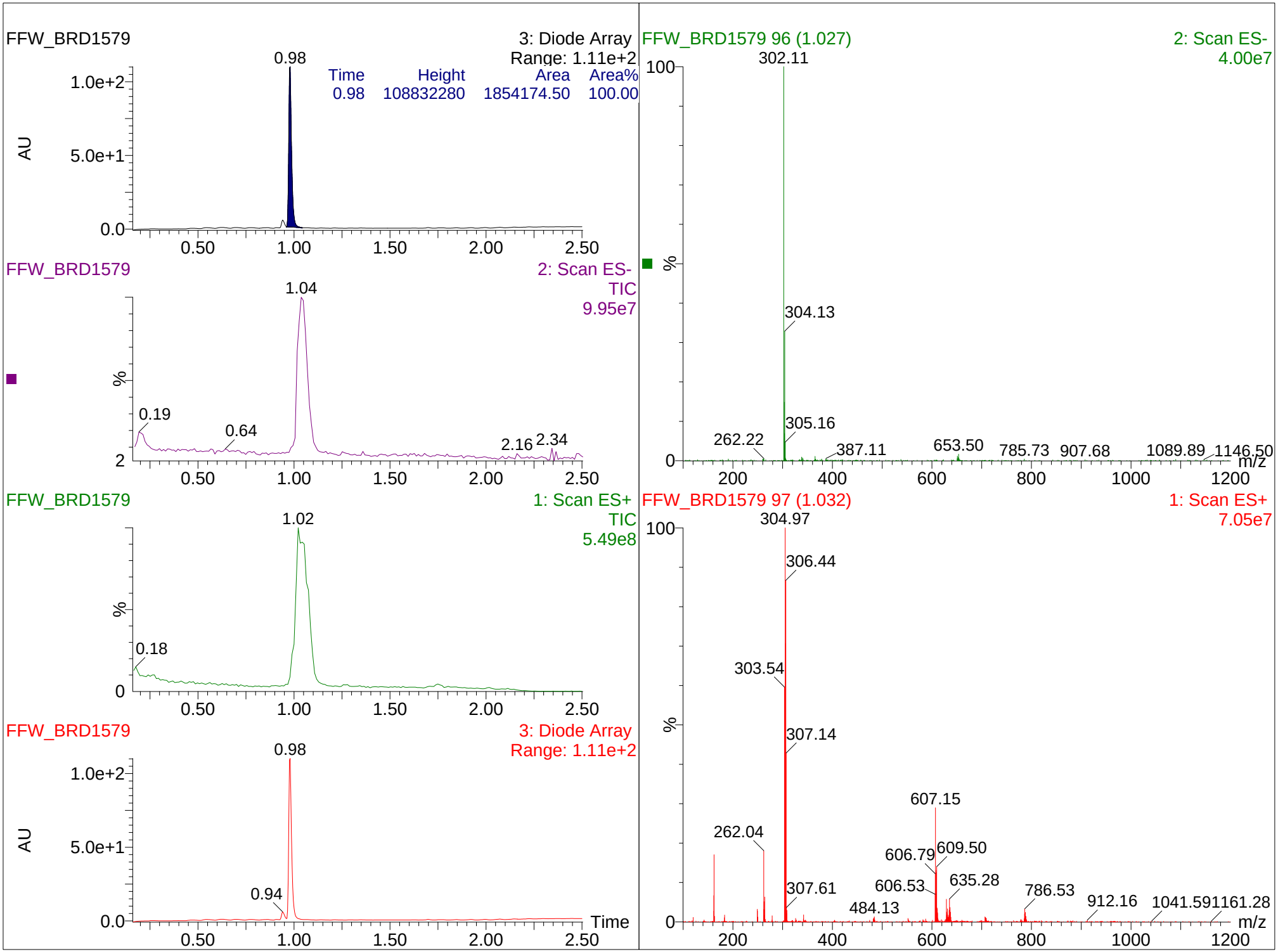
FFW_BRD1579
3: Diode Array
Range: 1.11e+2
0.98
Time Height Area Area%
0.98 108832280 1854174.50 100.00
AU
1.0e+2
5.0e+1
0.0
0.50 1.00 1.50 2.00 2.50
FFW_BRD1579
2: Scan ES-
TIC
9.95e7
1.04
%
0.19
0.64
2.16
2.34
2
FFW_BRD1579
1: Scan ES+
TIC
5.49e8
1.02
0.18
FFW_BRD1579
3: Diode Array
Range: 1.11e+2
0.98
0.94
Time
FFW_BRD1579 96 (1.027)
2: Scan ES-
4.00e7
302.11
100
304.13
305.16
262.22
387.11
653.50
785.73
907.68
1089.89
1146.50
m/z
200 400 600 800 1000 1200
FFW_BRD1579 97 (1.032)
1: Scan ES+
7.05e7
304.97
306.44
303.54
307.14
607.15
262.04
606.79
609.50
606.53
635.28
307.61
786.53
484.13
912.16
1041.59
1161.28

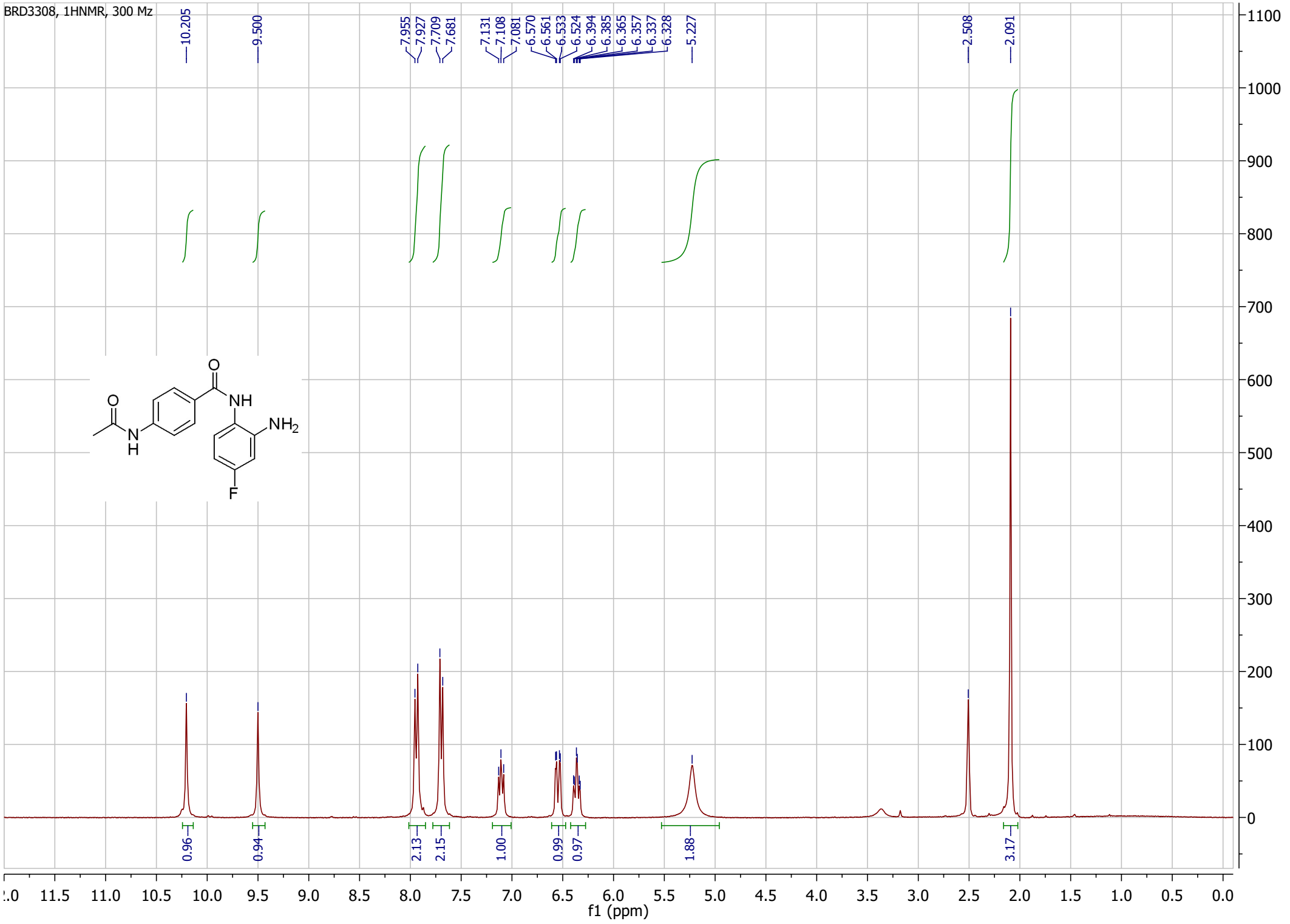
BRD3308, 1HNMR, 300 Mz
10.205
9.500
7.955
7.927
7.709
7.681
7.131
7.108
7.081
6.570
6.561
6.533
6.524
6.394
6.385
6.365
6.357
6.337
6.328
5.227
2.508
2.091
O
NH
NH2
O
N
H
F
0.96
0.94
2.13
2.15
1.00
0.99
0.97
1.88
3.17
f1 (ppm)

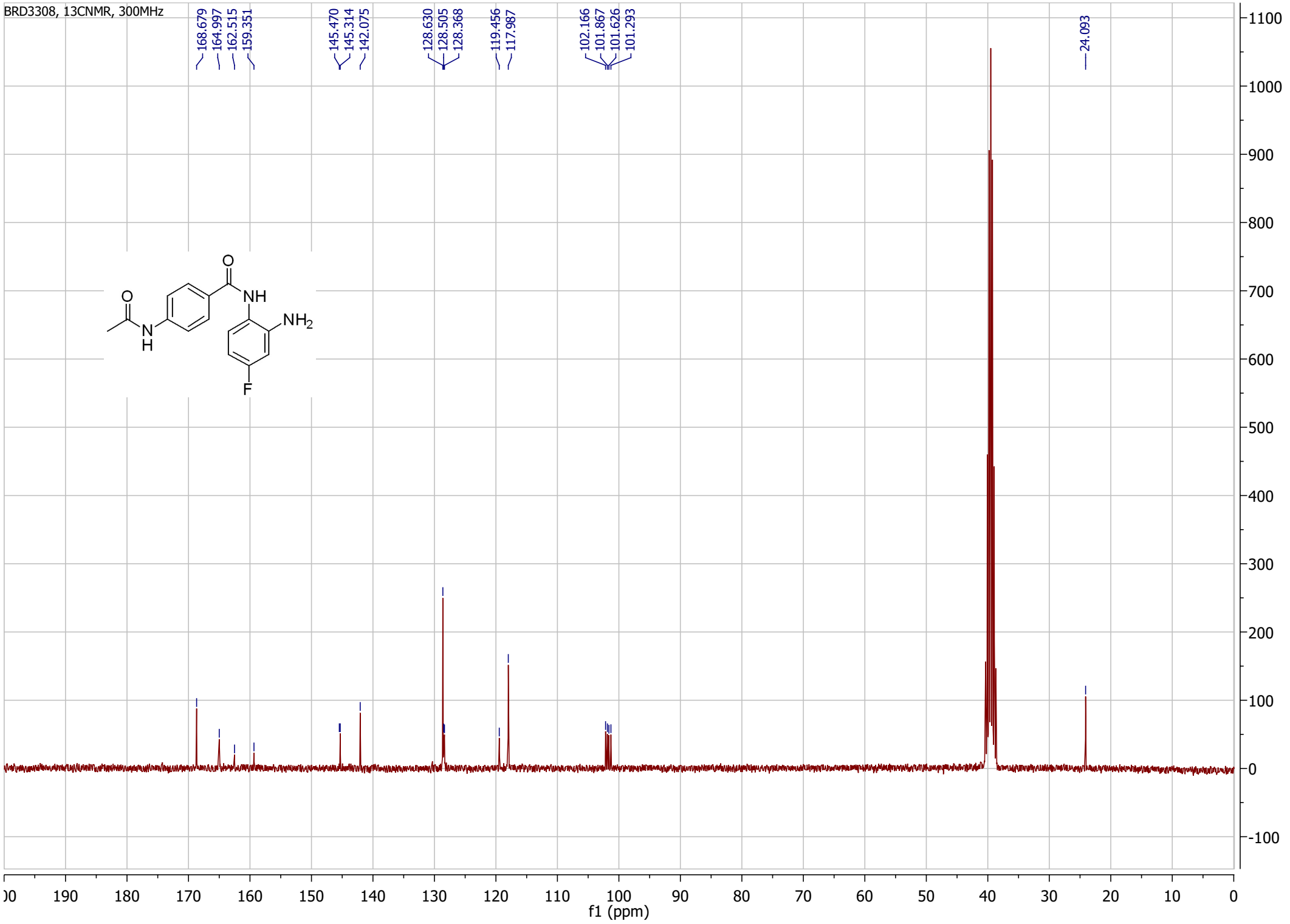
BRD3308, 13CNMR, 300MHz
168.679
164.997
162.515
159.351
145.470
145.314
142.075
128.630
128.505
128.368
119.456
117.987
102.166
101.867
101.626
101.293
24.093
O
NH
NH2
O
N
H
F
1100
1000
900
800
700
600
500
400
300
200
100
0
-100
190
180
170
160
150
140
130
120
110
100
90
80
70
60
50
40
30
20
10
0
f1 (ppm)

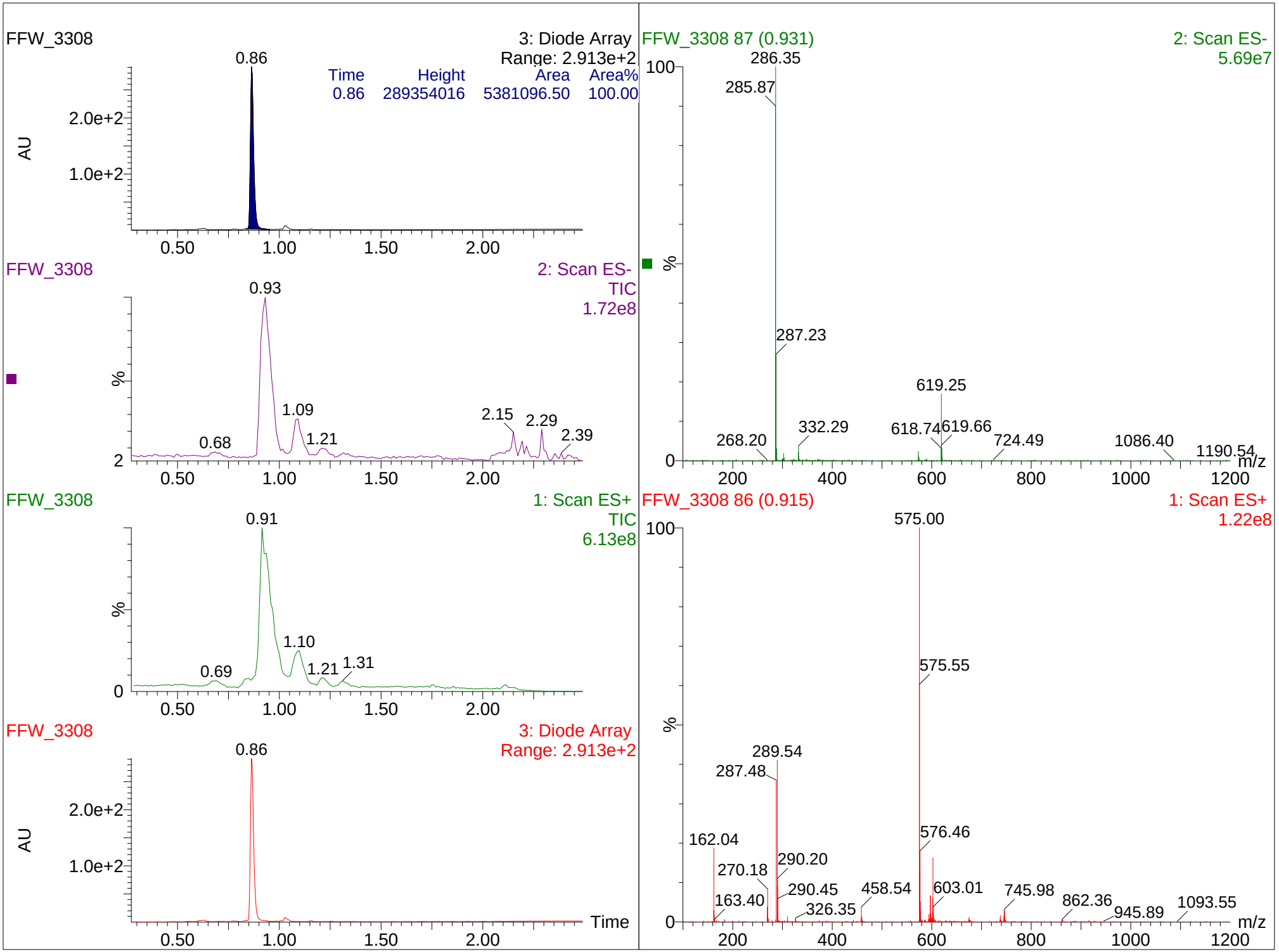
FFW_3308
3: Diode Array
Range: 2.913e+2
Time Height Area Area%
0.86 289354016 5381096.50 100.00
0.86
AU
2.0e+2
1.0e+2
0.50 1.00 1.50 2.00
FFW_3308
2: Scan ES-
TIC
1.72e8
0.93
1.09
1.21
0.68
2.15
2.29
2.39
%
2
0.50 1.00 1.50 2.00
FFW_3308
1: Scan ES+
TIC
6.13e8
0.91
1.10
1.21
1.31
0.69
%
0
0.50 1.00 1.50 2.00
FFW_3308
3: Diode Array
Range: 2.913e+2
0.86
AU
2.0e+2
1.0e+2
Time
0.50 1.00 1.50 2.00
FFW_3308 87 (0.931)
2: Scan ES-
5.69e7
286.35
285.87
287.23
619.25
332.29
618.74
619.66
268.20
724.49
1086.40
1190.54
100
%
0
200 400 600 800 1000 1200
m/z
FFW_3308 86 (0.915)
1: Scan ES+
1.22e8
575.00
575.55
289.54
287.48
576.46
162.04
290.20
270.18
290.45
458.54
603.01
745.98
862.36
945.89
1093.55
163.40
326.35
100
%
0
200 400 600 800 1000 1200
m/z